Liquid flow measurements in mountainstreams:

DILUTION METHOD FOR MEASUREMENT OF UNSTEADY FLOW USING BACK-INTO-TIME KALMAN FILTERING

August 1991

P. Vroege

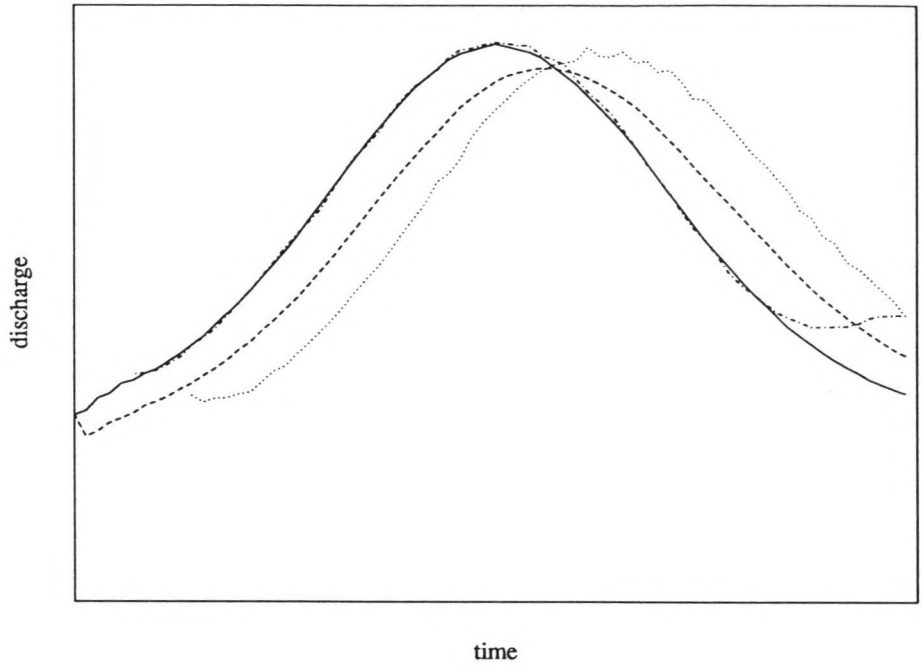

Technische Universiteit Delft
Faculteit der Civiele Techniek
Vakgroep Waterbouwkunde, k. 2.91
Stevinweg 1
2628 CN DELFT

TU Delft
Delft University of Technology

Faculty of Civil Engineering
Hydraulic and Geotechnical Engineering Division
Hydraulic and Offshore Engineering Section

Liquid flow measurements in mountain-streams :

DILUTION METHOD FOR MEASUREMENT OF UNSTEADY FLOW USING BACK-INTO-TIME KALMAN FILTERING

Peter Vroege

M.Sc. Thesis
August 1991

Thesis Supervisors :
Prof.dr. M. de Vries
Dr. H.L. Fontijn
Dr. Z.B. Wang

Delft University of Technology
Faculty of Civil Engineering
Hydraulic and Geotechnical Engineering Division
Hydraulic and Offshore Engineering Section

ACKNOWLEDGMENTS

This study is my M.Sc. thesis at the Faculty of Civil Engineering, Delft University of Technology.
I hereby wish to thank everyone who supported me during this study and especially my thesis supervisors Prof.dr. M. de Vries, dr. H.L. Fontijn and dr. Z.B. Wang for their active support, encouragement and valuable suggestions. Special thanks also go to my parents for their understanding and (financial) support.

Peter Vroege
August 1991

SUMMARY

In steady flow a well known method to determine a discharge is the method of dilution discharge-measurement : after constant injection of a known rate of tracer material and sufficient mixing over the entire cross-section, the concentration of the tracer material can be used to compute the discharge by way of an explicit relation.

Using the same relation during a flood wave (unsteady flow) will result in inaccurate values of the discharge caused by a difference in the respective velocities of propagation between flood wave and tracer cloud.

When, however, the dispersion equation is solved back into time with the aid of a Kalman filter, it turns out to be possible to compute with the dilution method accurate values of the discharge during a flood wave.

TABLE OF CONTENTS

CHAPTER 1 INTRODUCTION

To solve river engineering problems, it is in general necessary to have information on the characteristics of the river in question. One of these characteristics is the stage-discharge relationship. Several measurement techniques have been developed to measure the discharge, e.g. the velocity-area method, the moving boat method, the slope-area method, etc. Besides discharge measurement-structures can be used such as weirs and flumes. Many methods are described in detail in ISO (1990). A special method is the one of the dilution discharge-measurement. In principle this is a simple method : after constant injection of a known rate of tracer material and sufficient mixing over the entire cross-section, the concentration of the tracer material can be used to determine the discharge. The principle of this method is shown in Fig. 1-1.

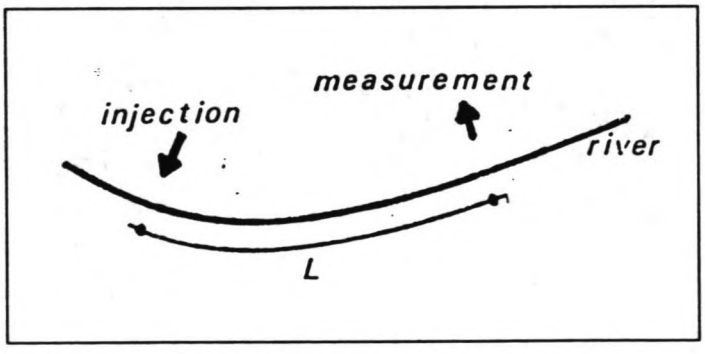

Fig. 1-1: Dilution method.

The necessity of mixing over the entire cross-section restricts the practical use of this method to small streams. So the dilution method seems to be particularly suitable for mountain-streams with excessive turbulence or debris, where the flow is inaccessible to man and/or measuring devices, or where the cross-sectional area cannot be accurately measured and current-meter measurements are impractical.
For steady flow the dilution method has been standardized by the International Standardization Organization (ISO, 1990), but for unsteady flow a sound theoretical background is still lacking.

This explains the aim of this study, viz. making the dilution method applicable for mountain-streams with a wild regime (excessive turbulence) under flood wave conditions (i.e. unsteady flow).
The problem of deriving the discharge from dilution measurements during flood-wave conditions has in principle been solved by Noppeney (1988). Noppeney has shown that a time lag (i.e. the result of a difference in the respective velocities of propagation between flood wave and tracer cloud) causes the major error in the computation of the discharge. Here the discharge was computed with the following expression :

$$\phi(L,t) = \frac{M}{Q(L,t)} + \phi_1 \qquad (1.1)$$

in which : $\phi(L,t)$ = concentration at x=L and time t,
ϕ_1 = initial (or 'background') concentration,
M = amount of released tracer material,
Q(L,t) = discharge at x=L and time t,
L = distance from injection point to point of measurement(L must be larger than the mixing length),
t = time.

The released tracer material is supposed to be a constant input, i.e. a constant amount of tracer material is continuously injected.
To avoid the error caused by the time lag, in this study a method is developed to compute the concentration at the injection point. Using again Eq. (1.1), but now for x=0, the discharge then can be computed.
Before developing this model a brief review of the theory of mixing processes in rivers is given in Chapter 2; a numerical approach to the dispersion equation is dealt with in Chapter 3.
The deterministic equations from Chapter 3 have to be matched with on-line measurements and one way to achieve this is the application of a Kalman filter. This is a stochastic filter based on a deterministic model and it has the capability of correcting model predictions using on-line information. An introduction to the Kalman filtering theory is given in Chapter 4 .
Chapter 5 contains the actual model to compute the concentration at the injection point; to this end a Kalman filter is developed based on

solving the difference equation back into time.

The performance of this filter is examined with simulated data in Chapter 6.

The conclusions which can be drawn and some recommendations for further study are given in Chapter 7.

CHAPTER 2 MIXING PROCESSES IN RIVERS

2.1 Introduction

In this Chapter a brief review of the theory of mixing processes in rivers is given. In Section 2.2 the dispersion equation is derived and in Section 2.3 the analytical solution for a steady uniform flow is given. In Section 2.4 the equation will be extended for rivers with dead zones.

2.2 Dispersion

The spreading of a dissolved substance in a turbulent open channel flow is due to a combined effect of diffusion and dispersion. An order of magnitude analysis indicates that dispersion by cross-sectional non-uniformity exceeds turbulent diffusion by far (e.g. Jansen, 1979). Dispersion has been defined as the spreading of marked fluid elements by the combined action of a velocity distribution and turbulent velocity fluctuations (Fig. 2-1).

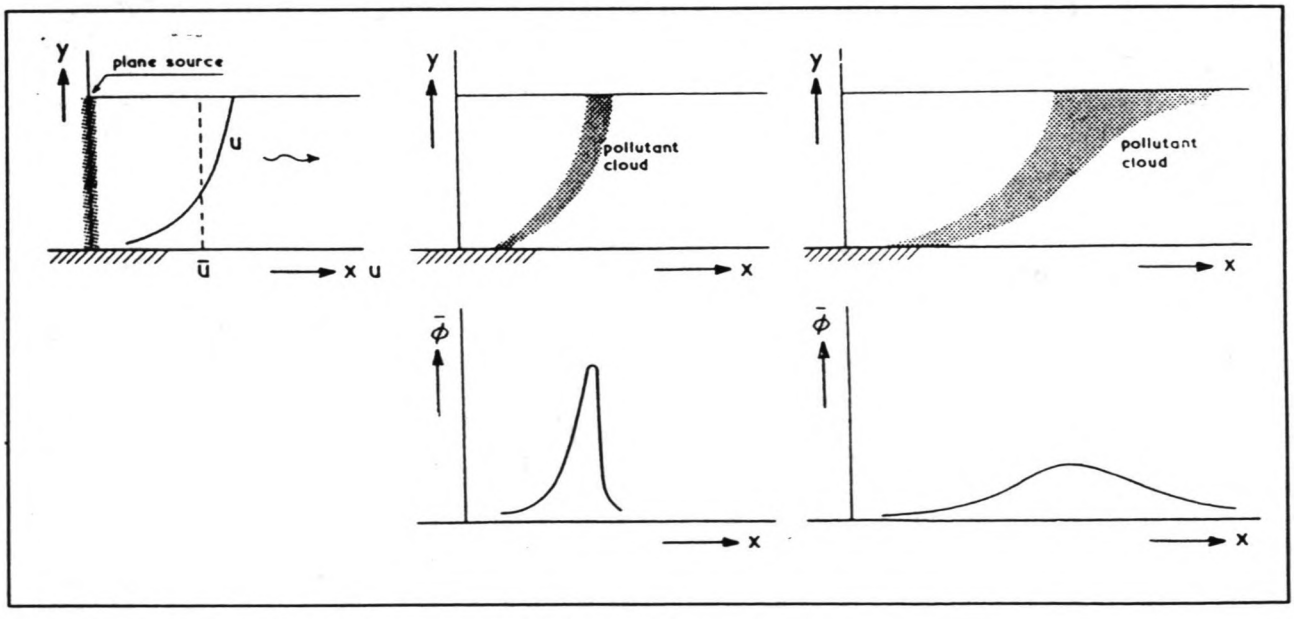

Fig. 2-1: Dispersion mechanism (after Fisher, 1979).

The basic one-dimensional differential equation for dispersion in channel flow is (see Noppeney, 1987):

$$\frac{\partial}{\partial t}\left(A\,\overline{\overline{\phi}} \right) + \frac{\partial}{\partial x}\left(A\overline{\overline{u}}\,\overline{\overline{\phi}} \right) + \frac{\partial}{\partial x}\left(A\,\overline{\overline{u''\phi''}} \right) = 0 \qquad (2.1)$$

in which : A = cross-sectional area of the river
u = flow velocity in x-direction
ϕ = concentration.

A double overbar denotes cross-sectional average and " stands for the turbulent and cross-sectional fluctuations with regard to this average, so

$$\phi = \phi(x,y,z,t) = \overline{\overline{\phi}}(x,t) + \phi''(x,y,z,t) \quad \text{with } \overline{\overline{\phi}}(x,t) = \frac{1}{A}\iint_A \phi \; dydz.$$

A similar expression holds for u.
A general procedure to express the last term in Eq. (2.1) in terms of a cross-sectional average is not available, but widely used in river engineering is the Taylor method.
Taylor (1954) assumed a balance between longitudinal convective transport and cross-sectional diffusive transport (Fig. 2-2), yielding the following relationship :

$$A\overline{\overline{u''\phi''}} = - AK \frac{\partial \overline{\overline{\phi}}}{\partial x}$$

in which : $K = - \frac{1}{A}\iint_A u''f(y,z)dydz$ = dispersion coefficient.

The function f(y,z) is defined by : $\phi'' = f(y,z)\,\frac{\partial \overline{\overline{\phi}}}{\partial x}$.
Substituting these expressions into Eq. (2.1) and omitting the overbars for simplicity yields the dispersion equation :

$$\frac{\partial}{\partial t}(A\phi) + \frac{\partial}{\partial x}(Au\phi) - \frac{\partial}{\partial x}\left(AK\frac{\partial \phi}{\partial x}\right) = 0 \qquad (2.2)$$

On account of laboratory and field experiments the dispersion coefficient for real streams is found to be (Fischer, 1979):

$$K = 0.011\,\frac{u^2B^2}{a\,u^*} \qquad (2.3)$$

in which : u^* = shear velocity

B = mean flow width

a = mean flow depth.

In most cases Eq. (2.3) has been found to agree within a factor 4, but 'a mountain stream that consist of a series of pools and riffles is not a suitable place to apply Taylor's analysis' (Fischer, 1979).

Day (1975) for example investigated the longitudinal dispersion of fluid particles in natural channels in an extensive series of experiments in small mountain streams in New Zealand. He concluded that the spread or standard deviation of an initially concentrated mass increases linearly with distance and not as its square root, as is necessary for the application of Taylor's mixing model. One consequence of this linearity is an ever-increasing dispersion coefficient along the channel.

Day also showed that the time-concentration curve of a dispersing tracer mass maintains a persistent asymmetry. This persistent asymmetry and the continued lineair spreading appear to be characteristic of dispersion in natural channels and as such show the inadequacies of applying Taylor's analysis.

However, since a better theory is not available the dispersion equation, Eq. (2.2), will be applied keeping in mind the imperfection of the theory.

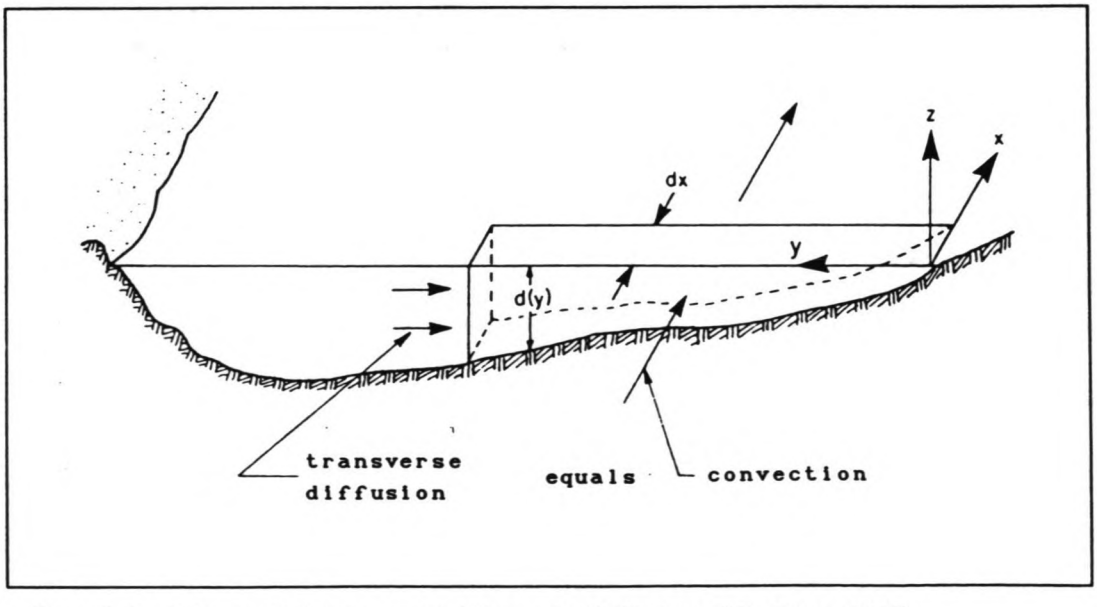

Fig. 2-2: Balance between convection and diffusion (Fischer, 1979).

2.3 Steady uniform-flow dispersion

For steady uniform flow the dispersion equation can be simplified to :

$$\frac{\partial \phi}{\partial t} + u \frac{\partial \phi}{\partial x} - K \frac{\partial^2 \phi}{\partial x^2} = 0 \qquad (2.4)$$

Assuming that at time t=0 there is no tracer material in the channel yields the initial condition :

$$\phi(x,0) = 0.$$

One boundary condition follows from reasoning that at infinity the concentration equals the initial concentration :

$$\lim_{x \to \pm\infty} \phi = 0.$$

For an impuls input at x=0 and t=0, the solution of the dispersion equation is given by (see e.g. de Vries, 1984) :

$$\phi(x,t) = \frac{M/A}{2\sqrt{\pi K t}} \exp\left[-\left(\frac{x-ut}{2\sqrt{Kt}}\right)^2\right] \qquad (2.5)$$

The concentration distribution for a constant input from t=0 at x=0 can be seen as the sum of the concentration distributions resulting from a successive series of impuls inputs during the time t (see Noppeney, 1987). This yields :

$$\phi(x,t) = \int_0^t \frac{M/A}{2\sqrt{\pi K \tau}} \exp\left[-\left(\frac{x-u\tau}{2\sqrt{K\tau}}\right)^2\right] d\tau \qquad (2.6)$$

This integral can be written as (Abramowitz and Stegun, 1965), see also Fig. 2-3 :

for x>0 :

$$\phi(x,t) = \frac{M}{2Au}\left[\operatorname{erf}\left(\frac{ut-x}{2\sqrt{Kt}}\right) - 1 + \exp\left(\frac{ux}{K}\right)\left(\operatorname{erf}\left(\frac{x+ut}{2\sqrt{Kt}}\right) + 1\right)\right]$$

for x<0 : (2.7)

$$\phi(x,t) = \frac{M}{2Au}\left[\operatorname{erfc}\left(\frac{x-ut}{2\sqrt{Kt}}\right) - \exp\left(\frac{ux}{K}\right)\operatorname{erfc}\left(\frac{x+ut}{2\sqrt{Kt}}\right)\right]$$

in which :

$$\mathrm{erf}(z) = \frac{2}{\sqrt{\pi}} \int_0^z \exp(-\sigma^2)d\sigma$$

$$\mathrm{erfc}(z) = 1 - \mathrm{erf}(z) = \frac{2}{\sqrt{\pi}} \int_z^\infty \exp(-\sigma^2)d\sigma$$

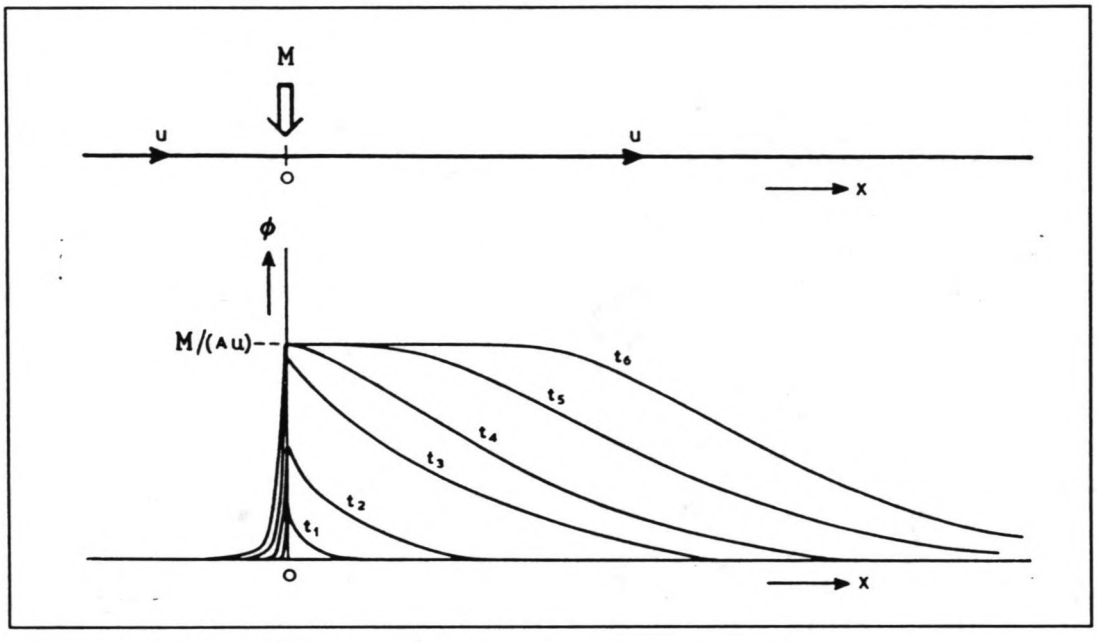

Fig. 2-3: Concentration distribution (Berkhoff, 1973).

2.4 Dead-zone model

In the cross-section of natural streams or rivers are parts where the water barely moves or parts with no net downstream movement. These 'dead zones' are quite arbitrarily distributed along the cross-section and may have a natural cause (e.g. due to meandering of the river, existence of debris, eddies or pockets behind obstacles like big rocks) or an artificial cause (like groynes or forelands).
When a tracer is injected into a river, tracer material will be trapped in these dead zones and this will have influence on the concentration distribution of the tracer.
The trapping of material in dead zones can be seen as a mass transport

through an interface between the flow and the dead part of the cross-section.
The transport of mass through the interface will, by complete mixing in the dead zone, be proportional to the difference in concentration between both zones :

$$F = - D (\phi_s - \phi_d)$$

in which : F = mass-flux through the interface
D = exchange velocity
index s : denotes the flow zone
d : denotes the dead zone

The value of the exchange velocity will be influenced by the cross-sectional geometry and the transport processes.
For the flow zone the dispersion equation can be extended to (see Noppeney, 1988) :

$$\frac{\partial \phi_s}{\partial t} + u_s \frac{\partial \phi_s}{\partial x} - K_s \frac{\partial^2 \phi_s}{\partial x^2} = - D_s (\phi_s - \phi_d) \qquad (2.8a)$$

while for the dead zone the equation becomes :

$$\frac{\partial \phi_d}{\partial t} = D_d (\phi_s - \phi_d) \qquad (2.8b)$$

in which the entrainment coefficients D_s and D_d are defined as :

$$D_s = \frac{P}{A_s} D \qquad , \qquad D_d = \frac{P}{A_d} D$$

with P = length in cross-section along which flow and dead zone make contact.

The storage time $1/D_d$ is the time tracer material stays in the dead zone and the relation between the two entrainment coefficients is :

$$D_s = \frac{A_d}{A_s} D_d$$

Thackston and Schnelle (1970) have found an experimental relation for the fraction of natural dead zones in a cross-section (see Fig. 2-4) :

$$\frac{A_d}{A_s + A_d} = 0.0152 + 0.89\ f^{2.22}$$

where f = friction factor and $0.04 < f < 0.26$.

Others like Purnama (1988) and Nordin and Troutman (1980) give a value in the order of $A_d/A_s \approx 0.03$.

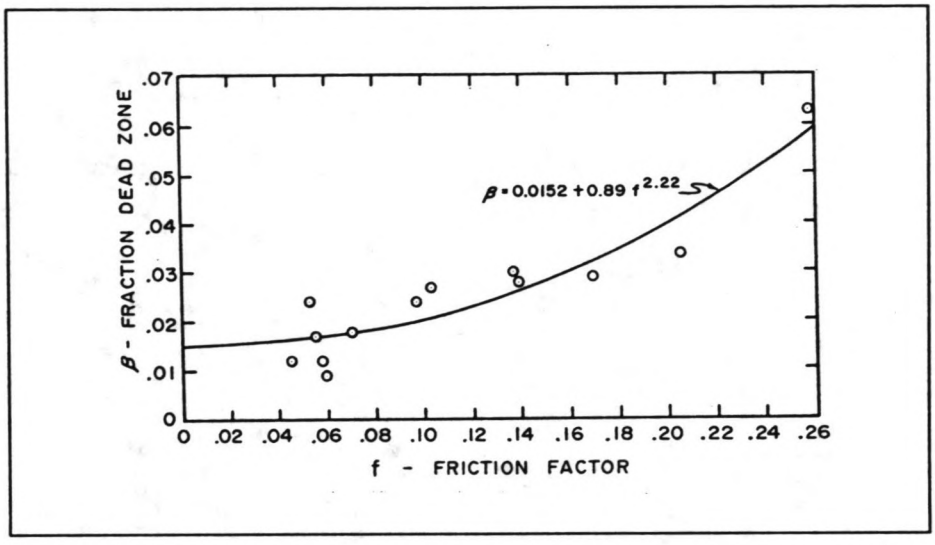

Fig. 2-4: Natural dead zone fraction (Thackston and Schnelle, 1970).

The dead-zone model generates an asymmetrical concentration distribution and with well-chosen parameters this model can lead to astonishing results as can be seen in Fig. 2-5.

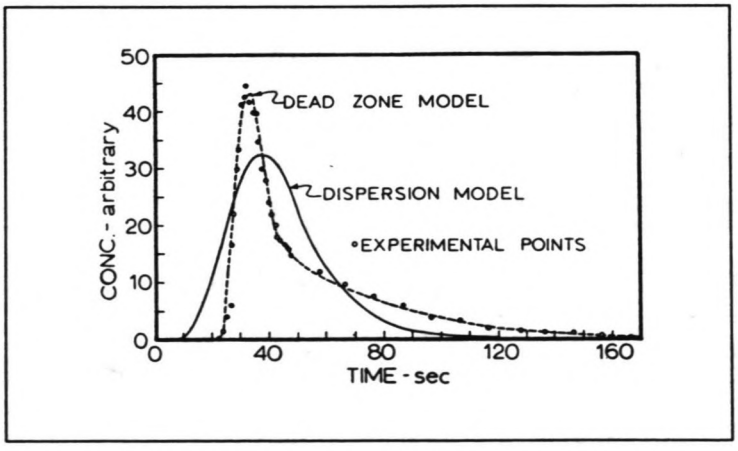

Fig. 2-5: Fit of two models to experimental data (Thackston and Schnelle, 1970).

CHAPTER 3 NUMERICAL APPROACH TO THE DISPERSION EQUATION

3.1 Introduction

A vast number of computational methods on dispersion are available and it is unfeasible trying to find the best. It is more important to avoid an uncritical use of the chosen scheme. Section 3.2 gives the numerical scheme that has been used for this study. The initial and boundary conditions needed to start a computation and to solve the difference equations are treated in Section 3.3. Section 3.4 contains some reflections on the accuracy of the numerical scheme.

3.2 Numerical scheme

The numerical scheme used to compute the solution of the dispersion equation, Eq. (2.4), is a finite difference scheme of the Crank-Nicholson type. Fig. 3-1 shows the definition of the grid.
The difference equation reads :

$$\frac{\phi_i^{k+1} - \phi_i^k}{\Delta t} + \theta \left\{ u \frac{\phi_{i+1}^{k+1} - \phi_{i-1}^{k+1}}{2\,\Delta x} - K \frac{\phi_{i+1}^{k+1} - 2\phi_i^{k+1} + \phi_{i-1}^{k+1}}{\Delta x^2} \right\} + \\ + (1-\theta) \left\{ u \frac{\phi_{i+1}^{k} - \phi_{i-1}^{k}}{2\,\Delta x} - K \frac{\phi_{i+1}^{k} - 2\phi_i^{k} + \phi_{i-1}^{k}}{\Delta x^2} \right\} = 0 \qquad (3.1)$$

in which : θ = weighting factor

ϕ_i^k = approximation of $\phi(i\Delta x, k\Delta t)$.

For $\theta > 0$ this is an implicit scheme and for $0.5 \leq \theta \leq 1$ the stability will be ensured without restrictions concerning the time step.

By defining $\underline{x} = \left[\phi_0^k \ldots \phi_i^k \ldots\right]^T$, where ^{T} denotes the transpose vector, the difference equation can symbolically be written as :

$$A\underline{x}_{k+1} = B\underline{x}_k + \underline{u}_{k+1}$$

where A and B are coefficient matrices and $\underline{u}_k$ depends on the boundary condition.

This can be rewritten as :

$$\underline{x}_{k+1} = \Phi\underline{x}_k + A^{-1}\underline{u}_{k+1} \qquad (3.2)$$

where $\Phi = A^{-1}B$.

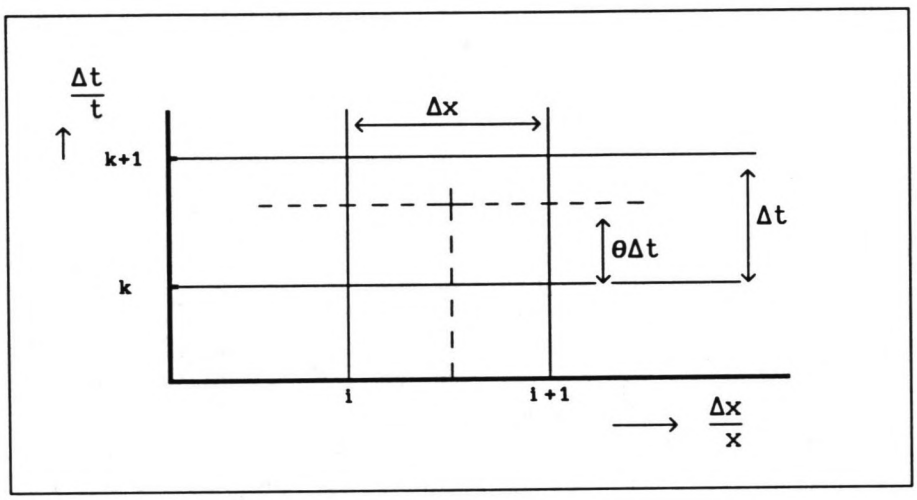

Fig. 3-1: Grid for finite difference scheme.

3.3 Initial and boundary conditions

Solving the above difference equation requires one initial and two boundary conditions.

As initial condition a constant background concentration ϕ_i throughout the channel is applied.

At the upstream boundary (x=0) the tracer input can be specified as a mass-flux with the following equation:

$$\phi(0,t) - K/u \frac{\partial\phi(0,t)}{\partial x} = \frac{M}{Q} H(t) + \phi_i \qquad (3.3)$$

or with the more simple concentration-condition, defined by :

$$\phi(0,t) = \frac{M}{Q} H(t) + \phi_i \qquad (3.4)$$

in which : $\phi(0,t)$ = concentration at the boundary

$H(t)$ = Heaviside or unit step function, defined as :

$$H(t) = 0 \quad \text{for } t<0$$
$$H(t) = 1 \quad \text{for } t>0$$

At the downstream boundary the model uses $\frac{\partial^2 \phi}{\partial x^2} = 0$ as a boundary condition.

3.4 Accuracy

In order to study the accuracy of the numerical solution of the dispersion equation it is for practical purposes often sufficient to consider the numerical dispersion, the numerical diffusion and the effects of the convection separately. If separate analyses of these phenomena yield reasonable accuracy for a given Δx, Δt and θ, it may be expected that the accuracy as a whole is acceptable (Vreugdenhil, 1989).

Numerical dispersion caused by the difference scheme can be quantified by expanding each difference term in a Taylor series. This yields the 'modified' equation and the 'modified' equation for the Crank-Nicholson scheme, Eq. (3.1), reads (e.g. Vreugdenhil, 1989) :

$$\frac{\partial \phi}{\partial t} + u \frac{\partial \phi}{\partial x} - K \frac{\partial^2 \phi}{\partial x^2} = (\theta-1/2)\ \Delta t\ u^2 \frac{\partial^2 \phi}{\partial x^2} + O(\Delta x^2, \Delta t^2)$$

The right hand side of this 'modified' equation is the truncation error and its first term has the nature of a dispersion coefficient (e.g. Vreugdenhil, 1989) :

$$K_{num} = (\theta-1/2)\ \Delta t\ u^2.$$

Apparently the computation is carried out with an effective dispersion coefficient :

$$K_{eff} = K + K_{num}.$$

This has two consequences. For reasons of stability the effective

dispersion coefficient should not be negative and for reasons of accuracy the numerical dispersion should be an order of magnitude smaller than the physical dispersion.
It has to be emphasized, however, that the other term in the truncation error may be important as well, but is more difficult to interpret.

The accuracy of the finite difference method for mere diffusion, can be judged by considering the diffusion equation as a 'black box', which transfers a certain 'input signal' at one location to an 'output signal' at another (e.g. Vreugdenhil, 1989). The difference between the respective transfer functions of the differential and the difference equation during, for example, the relaxation time yields a measure for the accuracy. This is given in Fig. 3-2 as function of θ, K, k and Δt, where k is the wave number of the wave present in the initial condition.

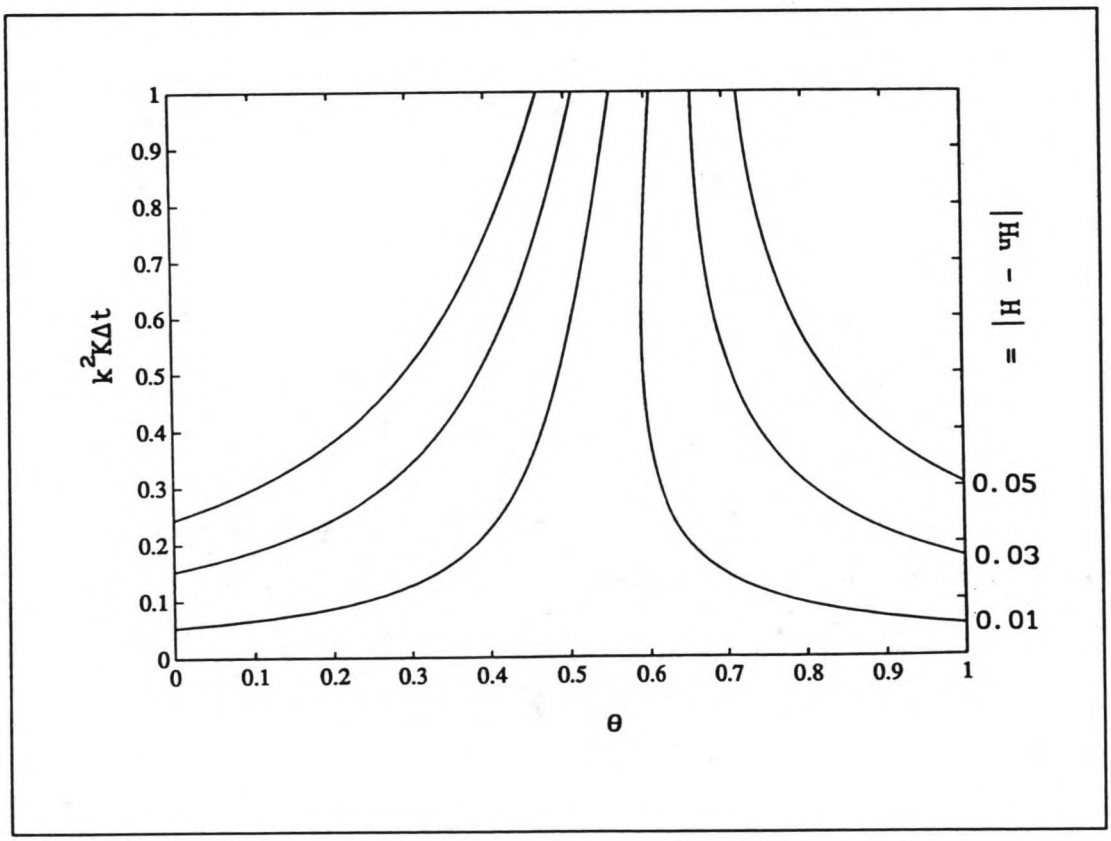

Fig. 3-2: Needed time-step for different levels of accuracy (after Vreugdenhil, 1985).

The influence of convection can be estimated by comparing propagation and damping by the differential and the difference equation. In Fig. 3-3 the relative celerity c_r (the ratio of the velocities of propagation) and damping factor d_n (the ratio of the amplitudes) are given as a function of $\Delta x/L$ and θ, where L is the wave length of the wave present in the initial condition.

In the case of a sudden variation in the concentration, e.g. imposed by a boundary condition or a sudden release of tracer, oscillations can occur even if the computational scheme is stable. The existance of these oscillations is governed by the cell-Peclet number P and a sufficient condition to prevent them is (e.g. Vreugdenhil, 1989) :

$$P = \frac{u\,\Delta x}{K} < 2.$$

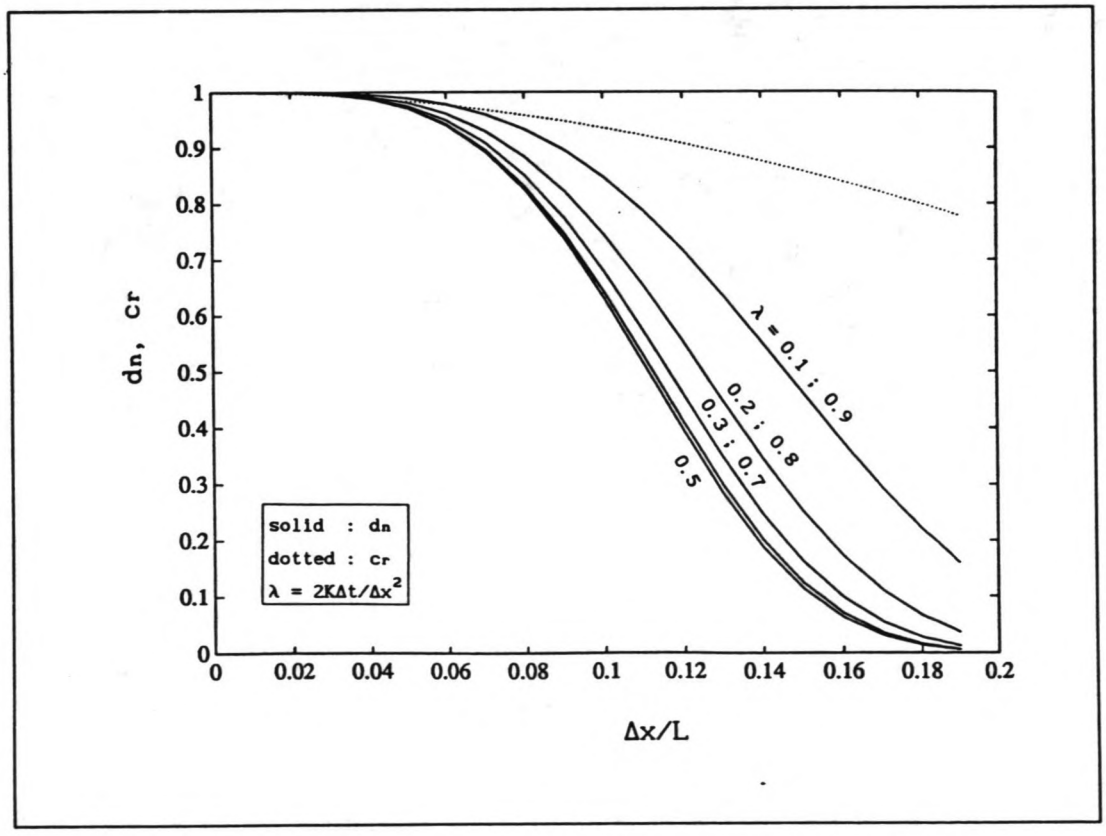

Fig. 3-3: Relative celerity and dampingfactor (after Noppeney, 1988).

CHAPTER 4 DISCRETE FILTERING THEORY

4.1 Introduction

Since the original papers by Kalman and Bucy (1960, 1961) a considerable amount of literature on the theory and the applications of Kalman filters has become available. In this chapter a short review of the filtering theory is given with special attention for those aspects of discrete filtering theory which are of major relevance to the problems dealt with in this study. For a more thorough discussion the reader is referred to the textbooks of Jazwinski (1970), Maybeck (1979, 1982) or Anderson and Moore (1979).

In Section 4.2 the Kalman filter for linear discrete systems is introduced and in Section 4.3 attention is paid to the stability of the filter. Section 4.4 gives an extension to nonlinear filters and Section 4.5 briefly discusses the use of the nonlinear filters in estimating uncertain parameters.

4.2 Linear filtering theory

The discussion of linear filters starts with the definition of a system and of the state of a system. A system represents a part of the real world (here a river) and the state of a system describes the system at a certain time t (here the concentration distribution). The different components describing the state of a system can be ranged into a vector; the state vector.
The essence in filtering now is to get an optimal estimation of the state at time t on account of the available information.
Suppose that the sequence of states is the result of a process and that this process can be described with a mathematical (or numerical) model. The difference between the actual system and this mathematical (or numerical) model is then defined as the system noise.
This study is dealing with the dispersive processes in a river and the

state vector $\underline{X}_k$ at time $t=k\Delta t$ is here defined by :

$$\underline{X}_k = \left[\phi_0^k \ldots \phi_i^k \ldots \phi_N^k\right]^T$$

where N = number of grid points.

Using the numerical scheme given in Section 3.2, the stochastic state equation describing the propagation in time of the state vector $\underline{X}_k$ can be written as :

$$\underline{X}_{k+1} = \Phi\, \underline{X}_k + A^{-1}\underline{u}_{k+1} + G\, \underline{W}_{k+1} \qquad k = 1,2,\ldots \qquad (4.1)$$

where $\underline{W}_k$ is the system-noise vector and G is the noise input-matrix.

A linear filter has a predictor-corrector structure and can be characterized as follows (Fig. 4-1):

- the time-dependent variables, represented in the state vector, are computed one time step ahead with the state equation until a measurement is available,
- the filter compares the corresponding state variable(s) or combination of state variables with the measurement(s),
- an adaptation vector is computed by the filter and added to the state yielding a corrected state.

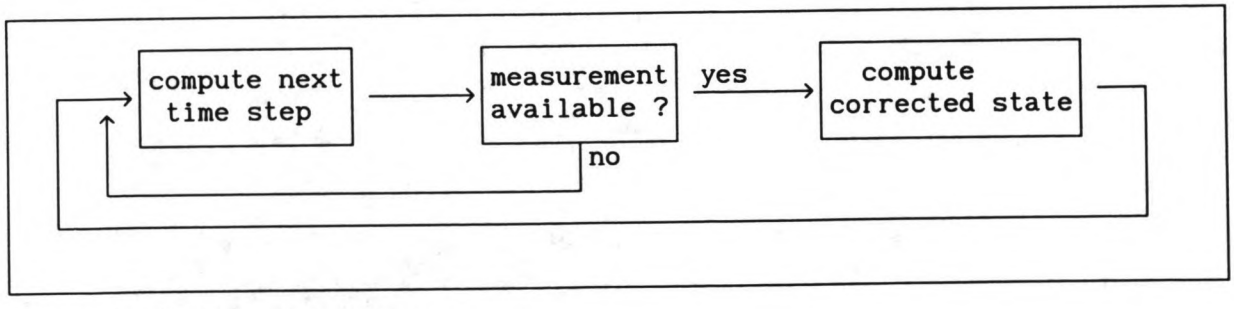

Fig. 4-1: Working of a filter.

To be able to compare the state vector with the available measurements, a relation between these two has to be formulated. This is done with the observation equation :

$$\underline{Z}_k = H\, \underline{X}_k + \underline{V}_k \qquad (4.2)$$

in which : $\underline{Z}_k$ = observation vector comprising the measurement(s) for $t = k\Delta t$,

H = observation matrix describing the actual relation(s) between state and measurement(s),

$\underline{V}_k$ = observation-noise vector, as all measurements will be disturbed with measurement faults.

Given the observations, the state equation and the observation equation the Kalman filter is able to give an optimal linear estimation of the state if the noise vectors are Gaussian white-noise processes. This means

$$E[\underline{W}_k] = \underline{q}_k = \underline{0} \qquad \text{and} \qquad E[\underline{V}_k] = \underline{r}_k = \underline{0}.$$

The covariance matrices of the system noise and the observation noise are defined as :

$$E[\underline{W}_k \, \underline{W}_k^T] = Q_k$$

$$E[\underline{V}_k \, \underline{V}_k^T] = R_k.$$

The Kalman filter for a discrete problem can be described by the following equations; the derivation of these filter equations can be found for instance in the works of Maybeck (1979) and Jazwinski (1970).

The prediction of the state is computed with :

$$\hat{\underline{X}}_{k+1} = \Phi \, \underline{X}_k + A^{-1} \underline{u}_{k+1} \tag{4.3}$$

where the circumflex ^ over a quantity denotes its predicted value.

The propagation of the covariance matrix P_k of the state $\underline{X}_k$ must also be computed, this is done through :

$$\hat{P}_{k+1} = \Phi \, P_k \, \Phi^T + G \, Q_{k+1} \, G^T \tag{4.4}$$

If an observation vector is available for the current time step (not necessarily every time step), the predicted state and covariance matrix are updated with the following corrector equations :

$$\underline{X}_{k+1} = \hat{\underline{X}}_{k+1} + K_{k+1} \left[Z_{k+1} - H \hat{\underline{X}}_{k+1} \right] \qquad (4.5)$$

$$P_{k+1} = \hat{P}_{k+1} - K_{k+1} H \hat{P}_{k+1} \qquad (4.6a)$$

or the numerically better equation (see Jazwinski, 1970, p.270) :

$$P_{k+1} = \left[I - K_{k+1} H \right] \hat{P}_{k+1} \left[I - K_{k+1} H \right]^T + K_{k+1} R_{k+1} K_{k+1}^T \qquad (4.6b)$$

in which :

$K_{k+1} = \hat{P}_{k+1} H^T \left[H \hat{P}_{k+1} H^T + R_{k+1} \right]^{-1}$ represents the Kalman gain, (4.7)

I = identity matrix,

$^{-1}$ denotes the matrix inverse.

A block-diagram representation of the Kalman filter described above is given in Fig. 4-2.

The initial conditions necessary to start the above Kalman filter are $\underline{X}_0$ and P_0.

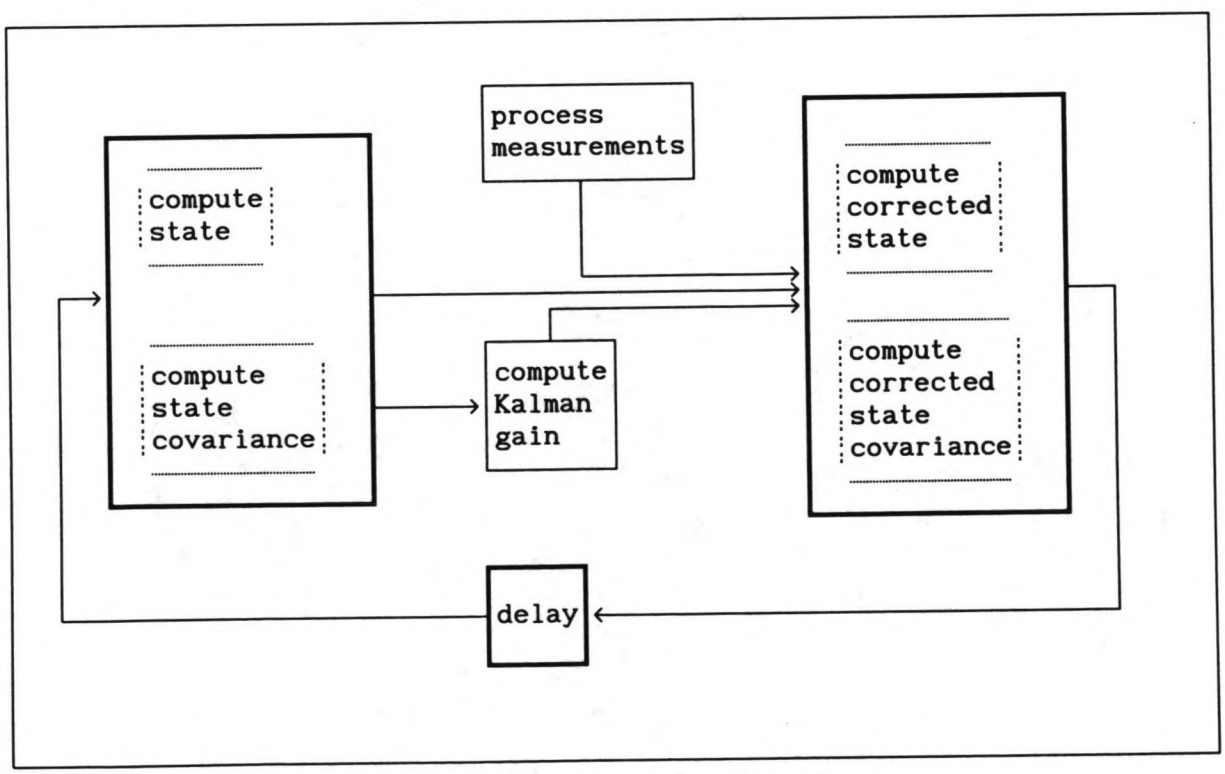

Fig. 4-2: Block-diagram representation of the Kalman filter.

4.3 Observability, controllability and stability

It is important to ask what, if anything, can be gained from filtering the data. How much information about the state of the system do the data contain? Can the state vector be determined from the data? The importance of these questions is obvious and if little is to be gained from filtering, remodelling the system should be considered. This might involve taking additional or alternative observations, or even redesigning the dynamics of the system.
How well the state is known is measured by the estimation-error covariance matrix P_k. Two concepts, the concept of observability and the concept of controllability, have been developed to check the condition of the filter (see Appendix A).

The concepts of observability and controllability, both introduced by Kalman, can be used to establish stability. Through the explicit generation of an appropriate Lyapunov function, it can be proved that, if a system model is both uniformly completely observable and controllable, the Kalman filter is uniformly exponentially stable (see Kalman, 1963).
An immediate consequence of the exponential stability of a filter is that the effect of the initial condition P_0 vanishes as more and more observations are incorporated. This is important, since P_0 is often poorly known. Furthermore, it indicates that the computation of P_k is stable and the numerical errors in P_k vanish (Heemink, 1986). This is a very favourable property, since in case the Kalman filter algorithm is applied to ill-conditioned problems, these numerical errors can become large.

Another approach to the stability of the filter can be obtained from the filter equations (4.3)-(4.7). It can be shown that for the model described in section 4.2 :

$$\| I - K(k)\, H(k) \| \leq 1 \qquad \text{, for all } k.$$

Here $\|\cdot\|$ denotes a matrix norm.

This implies that if the original system (4.1) is (exponentially) stable, the Kalman filter is also (exponentially) stable and that the filter is always more stable than the original system (Heemink, 1986). This stability-improvement property of the filter is a very favourable one. Note that if the filter is uniformly completely observable and controllable, stability of the original system is not required for filter stability. A system model can be unstable whereas the Kalman filter is stable.

4.4 Nonlinear filtering theory

This Section contains only a few remarks on the theory of nonlinear filtering. A more detailed discussion can be found in Appendix B.
The Kalman filter was originally derived for linear models only, but algorithms have been developed to linearize nonlinear models.
One way to linearize is using a reference trajectory along which the partial derivatives of the nonlinear equations are determined, yielding approximate linear equations which can be used in a standard Kalman filter.
The remaining problem is choosing the reference trajectory. The easiest way is to pick, a priori, a reference trajectory; this approach is called the Linearized Kalman filter. The performance of this Linearized Kalman filter depends, however, very strongly on the accuracy of the reference trajectory chosen.
A better method is the application of the Extended Kalman filter, where a new and better reference trajectory is incorporated into the estimation process as soon as a new observation is available and a new corrected state has been obtained. With this choice of reference trajectory large initial estimation errors are not allowed to propagate into time.

4.5 Parameter estimation

A particular application of nonlinear filters is the estimation of state variables in a system which is well described by a (non)linear model, but in which uncertain parameters are embedded in the Φ and/or H matrices. These uncertain parameters can be treated as additional state variables with the system equation :

$$\underline{P}_{tk} = \underline{P}_{tk-1} + \underline{W}p_{tk} \tag{4.8}$$

By incorporating the system noise $\underline{W}p_{tk}$ into this equation the random character of the parameters can be taken into account. Note that in general even a linear model in this case becomes a highly nonlinear one. By applying a nonlinear filter to estimate both the state and the uncertain parameters, it is possible to adapt the model to changing physical conditions. Compared to other methods for combined state and parameter estimation, this procedure is attractive from a computational point of view. Owing to the neglected higher-order nonlinearities, bias errors may also appear in the parameter estimation. The more pronounced the nonlinearities are, the more the filter performance is degraded by this effect. Therefore, in a given application the capability of the filter to estimate uncertain parameters has to be verified by applying the filter using simulated data. In that case the true value of the parameters is known and, consequently, the performance of the filter can be evaluated under a variety of circumstances.

CHAPTER 5 BACK-INTO-TIME MODEL

5.1 Introduction

In Chapter 3 a numerical scheme has been derived to compute the dispersion equation. This scheme needs the discharge at the upstream boundary, but this discharge is the quantity looked for and therefore not known.

If the dispersion equation is numerically solved with the aid of a Kalman filter, this problem can be avoided by considering the upstream boundary (x=0) concentration as an autoregressive variable, that is :

$$\phi_0^{k+1} = \phi_0^k \tag{5.1}$$

The general idea now is :

- inject the tracer at x=0 (= upstream boundary);
- measure the concentration of tracer material at x=L (=downstream boundary);
- compute the concentration at x=0;
- and finally, compute from this concentration the discharge with a normal boundary condition like the concentration condition, which is :

$$\phi(0,t) = \frac{M(t)}{Q(0,t)} + \phi_i$$

yielding :

$$Q(0,t) = \frac{M(t)}{\phi(0,t) - \phi_i} \tag{5.2}$$

Here we recall that :

$\phi(0,t)$ = concentration at the upstream boundary
ϕ_i = initial (or 'background') concentration
$M(t)$ = released tracer material
$Q(0,t)$ = discharge at the upstream boundary.

So the major problem is to regain the upstream boundary concentration given the measured downstream concentration. Therefore the numerical scheme from Section 3.2 combined with an autoregressive boundary as described above, is incorporated into a Kalman filter. This model is

tested with the aid of a simulated flood wave down an imaginary river. Fig. 5-1 shows the distribution of the concentration along the river at some time t after the release of the tracer at x=0 was started. The distribution computed with the model, where the concentration at x=L was inserted as measured concentration, is also given.

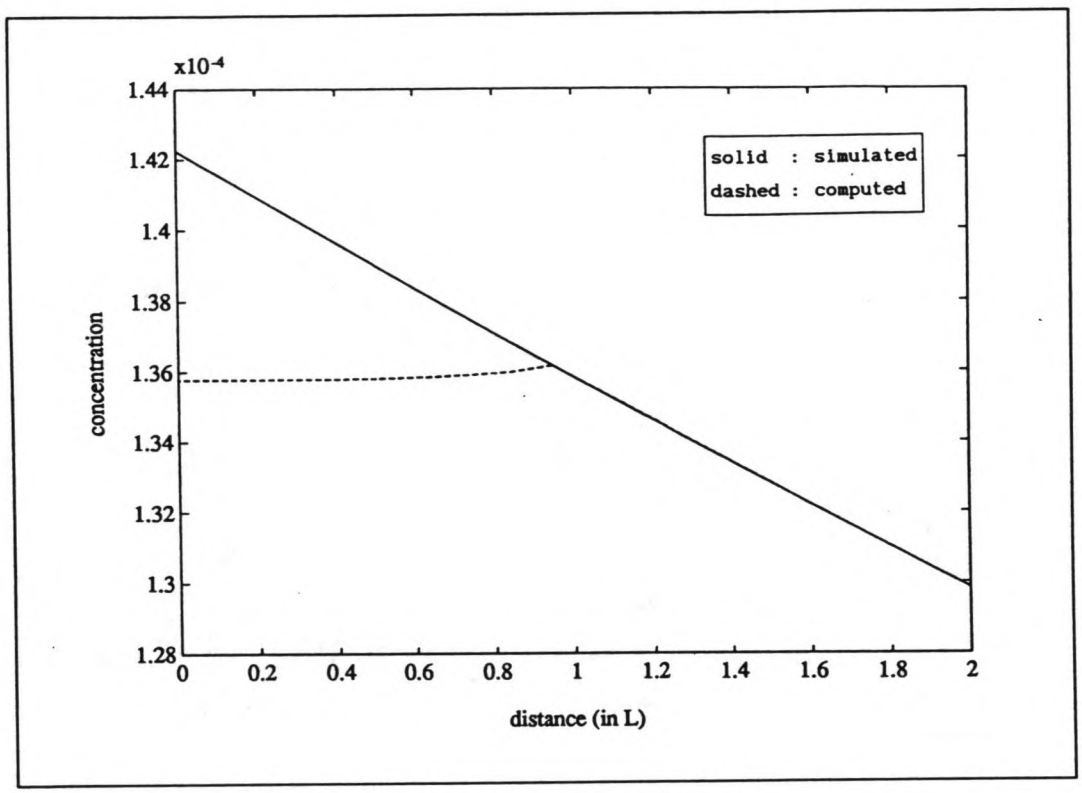

Fig. 5-1: Concentration computed with a Kalman filter.

It can clearly be seen that the model shifts the concentration at x=L to the 'measured' concentration, resulting in a fairly well computed concentration for x≥L (the Kalman filter actually introduces a new boundary condition at x=L).

Unfortunately, this is not what we are looking for; we want to find the upstream distribution of the concentration, and it is also clear that this model cannot provide that. This is not a real surprise if we take in mind that the concentration at x=L for the greater part contains information from the past and hardly information about the future.

Due to the fact that the present contains information about the past, we have chosen to solve the dispersion equation back into time, hoping to

find the boundary concentration that caused the measured concentration. To solve the dispersion equation (2.4), back into time an explicit finite difference scheme is used.
The difference equation reads :

$$\frac{\phi_i^{k+1} - \phi_i^k}{\Delta t} + u \frac{\phi_{i+1}^k - \phi_{i-1}^k}{2\,\Delta x} - K \frac{\phi_{i+1}^k - 2\phi_i^k + \phi_{i-1}^k}{\Delta x^2} = 0 \qquad (5.3)$$

When the boundary conditions are embedded into the system matrix Φ, this equation can be rewritten as :

$$\underline{X}_{k+1} = \Phi\, \underline{X}_k \qquad (5.4)$$

where $\underline{X}_k$ consists of the concentrations in the grid points :

$$\underline{X}_k = \left[\phi_0^k \ldots \phi_i^k \ldots \phi_N^k\right]^T$$

The concept of back-into-time solving, is to take the inverse of Eq. (5.4), so :

$$\underline{X}_k = F\, \underline{X}_{k+1} \qquad (5.5)$$

where $F = \Phi^{-1}$.

Although an analytically correct move, numerical instability may occur due to this inversion as will be shown in the next Section. Section 5.3 describes a Kalman filter based on the back-into-time scheme. The accuracy of the back-into-time method will be investigated in Section 5.4 and in Section 5.5 an extension for rivers with dead zones is given.

5.2 Stability of the back-into-time method

To study the stability of this back-into-time scheme, the Von Neumann method is used.
Suppose an initial condition of the form :

$$\phi_j^0 = \phi^0 \cos(kx)$$

For convenience' sake, this is written as :

$$\phi_j^0 = \phi^0 \exp(ij\xi) \qquad (5.6)$$

in which : ϕ^n = amplitude at time level n

i = complex number i

j = grid point number

$\xi = k\Delta x = 2\pi\Delta x/L$ (k = wave-number, L = wave length)

Obviously the smallest possible grid size is $\Delta x = 0$. The largest possible value is $\Delta x = L/2$, as it is not possible to represent a "wave" with less than two grid points per wave length.
So : $0 \leq \xi \leq \pi$.

Rewriting the difference equation (5.3) to :

$$\phi_j^{n+1} = \phi_j^n - \frac{u\Delta t}{2\Delta x}(\phi_{j+1}^n - \phi_{j-1}^n) + \frac{K\Delta t}{\Delta x^2}(\phi_{j+1}^n - 2\phi_j^k + \phi_{j-1}^k) \qquad (5.7)$$

and substituting Eq. (5.6) into Eq. (5.7) yields :

$$\phi^{n+1}\exp(ij\xi) = \phi^n\left\{1 - \frac{1}{2}\sigma\left[\exp(i(j+1)\xi) - \exp(i(j-1)\xi)\right] + \frac{1}{2}\lambda\left[\exp(i(j+1)\xi) - 2\exp(ij\xi) + \exp(i(j-1)\xi)\right]\right\} \qquad (5.8)$$

where $\sigma = u\Delta t/\Delta x$

$\lambda = 2K\Delta t/\Delta x^2$.

Each term in Eq. (5.8) contains a factor $\exp(ij\xi)$, therefore

$$\phi^{n+1} = \phi^n\left\{1 - \frac{1}{2}\sigma\left[\exp(i\xi) - \exp(-i\xi)\right] + \frac{1}{2}\lambda\left[\exp(i\xi) - 2 + \exp(-i\xi)\right]\right\} =$$

$$= \phi^n\left\{1 - \lambda + \lambda\cos(\xi) - \sigma\, i\sin(\xi)\right\} \qquad (5.9)$$

This equation can now easily be written in back-into-time form :

$$\phi^n = \frac{1}{1 - \lambda + \lambda\cos(\xi) - \sigma\, i\sin(\xi)}\,\phi^{n+1} \qquad (5.10)$$

The numerical solution has been multiplied during this time step by a complex factor : the amplification factor ρ

$$\rho = \frac{1}{1 + \lambda(\cos(\xi) - 1) - \sigma\, i\sin(\xi)} \qquad (5.11)$$

which means that the amplitude is multiplied by $|\rho|$ and that there is a phase shift $\arg(\rho)$. During the next time step the same will happen and after n time steps the multiplication factor is $|\rho|^n$.
Here we started with a cosine function as an initial condition, but any initial function can be developed into a Fourier series consisting of cosine functions with various wave lengths. So, apparently, a general condition for stability is that the absolute value of the amplification factor should be less than unity :

$$|\rho| \leq 1 \tag{5.12}$$

for any value of the wave length L and the grid size Δx.
Elaboration of Eq. (5.12) gives :

$$|\rho|^2 = \frac{1}{\left[1+\lambda(\cos(\xi)-1)\right]^2 + \sigma^2\sin^2(\xi)} \leq 1$$

$$2\lambda(\cos(\xi)-1) + \lambda^2(\cos(\xi)-1)^2 + \sigma^2(1-\cos^2(\xi)) \geq 0$$

Dividing by $(\cos(\xi)-1)$ yields :

$$2\lambda + \lambda^2(\cos(\xi)-1) - \sigma^2(1+\cos(\xi)) \leq 0$$

This is a linear function of $\cos(\xi)$, so if the inequality is satisfied for the two extreme values of $\cos(\xi)$, ± 1, it is for the intermediate values as well. This gives :

$$\cos(\xi) = 1 \longrightarrow 2\lambda - 2\sigma^2 \leq 0 \longrightarrow \lambda \leq \sigma^2$$

$$\cos(\xi) = -1 \longrightarrow 2\lambda - 2\lambda^2 \leq 0 \longrightarrow \lambda \geq 1$$

Combination of these two conditions gives the stability condition for the back-into-time scheme :

$$1 \leq \lambda \leq \sigma^2 \tag{5.13}$$

which is quite the opposite of the stability condition for the explicit Crank-Nicholson scheme, (see e.g. Vreugdenhil, 1989) :

$$\sigma^2 \leq \lambda \leq 1 \tag{5.14}$$

The meaning of this last condition is that Δx can be chosen and that then Δt is limited by Eq. (5.14) : the time step cannot be taken arbitrarily large. A way to get round this sometimes severe stability restriction is using an implicit method, which is unconditionally stable if $1/2 \leq \theta \leq 1$ (see Vreugdenhil, 1989).
The meaning of the stability condition for the back-into-time scheme,

Eq. (5.13), is that for a given time step Δt the grid size Δx is limited. With the Von Neumann method it can be proven that an implicit back-into-time scheme is unstable for $1/2 \leq \theta \leq 1$ and only conditionally stable for $0 \leq \theta \leq 1/2$, and these conditions are more severe than Eq. (5.13). Therefore only explicit schemes will be used for the back-into-time computation.

However, even when satifying condition (5.13), the back-into-time method appears to be unstable; oscillations originate at the downstream boundary, travel upstream and grow exponentially. These oscillations appear for every combination of σ and λ, and therefore it can be concluded that the back-into-time method is useless, unless a special way to stabilize the method can be found.
A stable method can be found by incorporating the back-into-time scheme into a Kalman filter, as can be seen in Fig. 5-2 where the effect of the Kalman filter on the oscillations can be seen quite clearly.

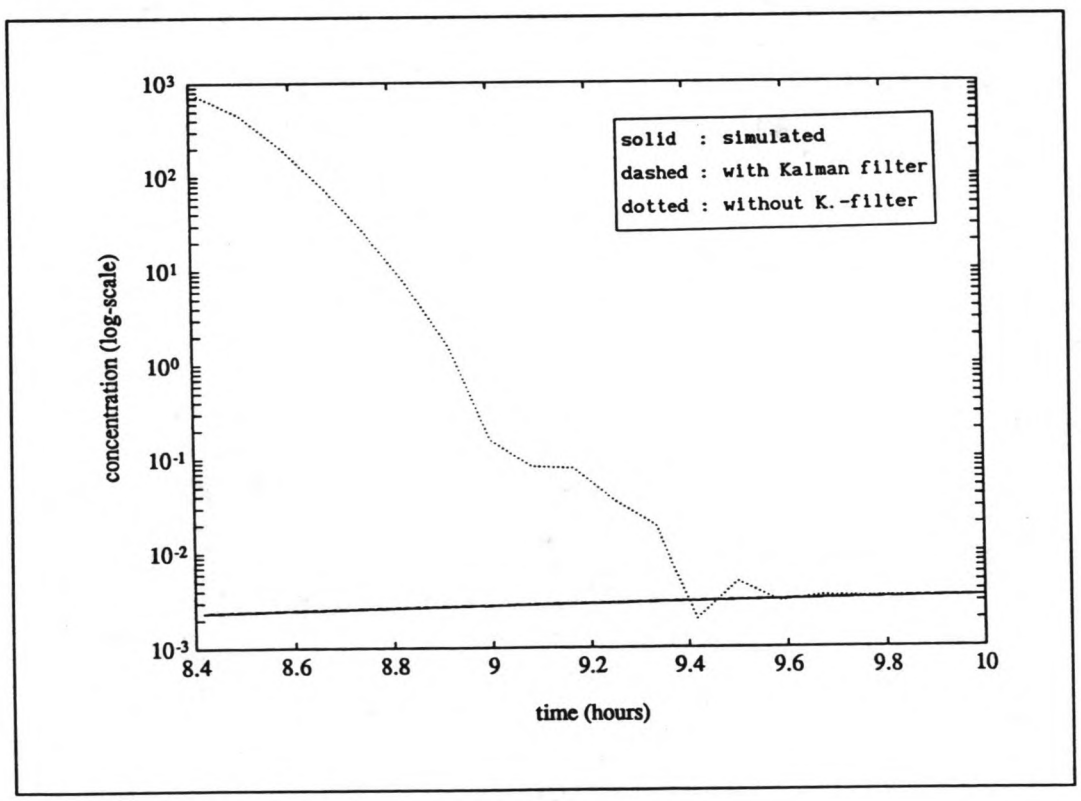

Fig. 5-2: Stabilizing effect of the Kalman filter.

5.3 A Kalman filter based on the back-into-time method

Before a Kalman filter can be applied, the deterministic equation (5.5) presented in Section 5.1 has to be converted into a stochastic equation. This can be done by assuming that the modelling errors can be caught into a noise vector and adding this noise vector to Eq. (5.5), yielding the following stochastic system equation :

$$\underline{X}_{tk} = F\,\underline{X}_{tk+1} + \underline{W}_{tk} \tag{5.15}$$

where $\underline{W}_{tk}$ = system-noise.

To be able to match the computed state $\underline{X}_{tk}$ with measurements, the Kalman filter needs another equation : the observation equation. This observation equation must give a relation between the state and the measurements. In our case this relation is quite simple, as one of the state variables is measured.

The observation equation can be written as :

$$\underline{Z}_{tk} = H\,\underline{X}_{tk} + \underline{V}_{tk} \tag{5.16}$$

where $\underline{V}_{tk}$ = observation-noise

H = observation matrix.

As only the concentration at the downstream boundary is measured, the observation matrix $H = [0\ ;\ \cdots\ ;\ 0\ ;\ 1]$.

The boundary conditions are embedded in the original system matrix Φ ($F = \Phi^{-1}$), where at the upstream boundary the concentration is considered to be an autoregressive variable, see Eq. (5.1); as downstream boundary $\partial^2\phi/\partial x^2 = 0$ is used.

The resulting system is :

$$\begin{pmatrix} \phi_0^k \\ \phi_1^k \\ \vdots \\ \phi_{N-1}^k \\ \phi_N^k \end{pmatrix} = \begin{pmatrix} 1 & 0 & 0 & 0 \\ \frac{1}{2}(\sigma+\lambda) & (1-\lambda) & \frac{1}{2}(-\sigma+\lambda) & 0 \\ & \ddots & \ddots & \ddots \\ 0 & \frac{1}{2}(\sigma+\lambda) & (1-\lambda) & \frac{1}{2}(-\sigma+\lambda) \\ 0 & 0 & \sigma & (1-\sigma) \end{pmatrix}^{-1} \begin{pmatrix} \phi_0^{k+1} \\ \phi_1^{k+1} \\ \vdots \\ \phi_{N-1}^{k+1} \\ \phi_N^{k+1} \end{pmatrix} + \underline{W}_{tk}$$

$$\underline{X}_{tk} = \phi^{-1}\,\underline{X}_{tk+1} + \underline{W}_{tk}$$

$$(\phi m_N) = [0 \cdots 0\ 1] \begin{pmatrix} \phi_0 \\ \vdots \\ \phi_N \end{pmatrix} + \underline{V}_{tk}$$

$$\underline{Z}_{tk} = H \underline{X}_{tk} + \underline{V}_{tk}$$

where N = number of grid points

ϕm = measured concentration.

5.4 Accuracy of the back-into-time method

In order to study the numerical accuracy for the back-into-time method, the numerical effects of diffusion and convection are considered separately (see Section 3.4).

For diffusion the transfer functions of the differential and the difference equations are needed. If as initial condition is taken

$$\phi(x,0) = \phi_0 \cos(kx)$$

Vreugdenhil (1989) gives for the differential equation :

$$\phi(x,t) = H\ \phi_0 \cos(kx)\ ,\ \text{with } H = \exp(-Kk^2t)$$

and for the difference equation :

$$\phi n(x,t) = Hn\ \phi_0 \cos(kx)\ ,\ \text{with } Hn = \rho^n = (1+\lambda(\cos(\xi)-1))^n$$

where $n=t/\Delta t$ is the number of time steps and ρ is the amplification factor of the numerical method used.

Rewriting this to back-into-time mode, yields :

$$\phi(x,0) = Ht\ \phi(x,t) = H^{-1}\phi(x,t)$$

$$\phi(x,0) = Htn\ \phi(x,t) = Hn^{-1}\phi(x,t)$$

In Fig. 5-3 the transfer functions H and Ht are given as function of the wave length k. It is clear that in the back-into-time scheme shorter waves are no longer damped out by diffusion. Fig. 5-4 gives the relative error for the back-into-time scheme as well as for the original scheme.

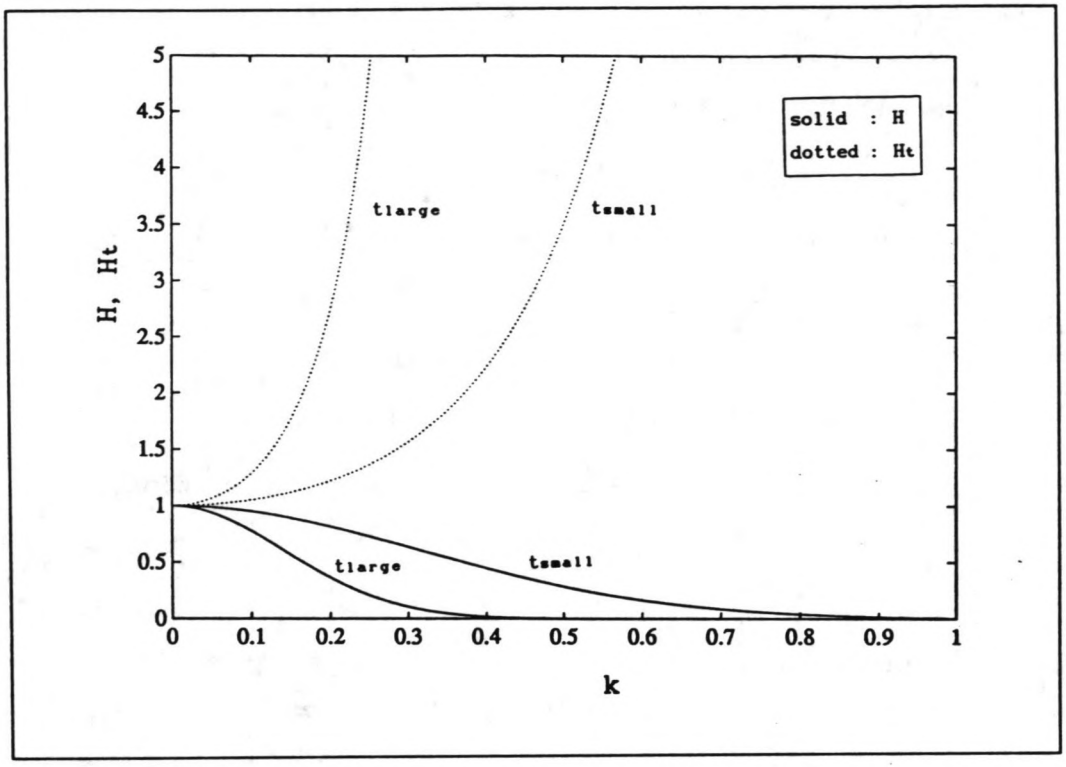

Fig. 5-3: Transfer functions for the diffusion equations (after Vreugdenhil, 1989).

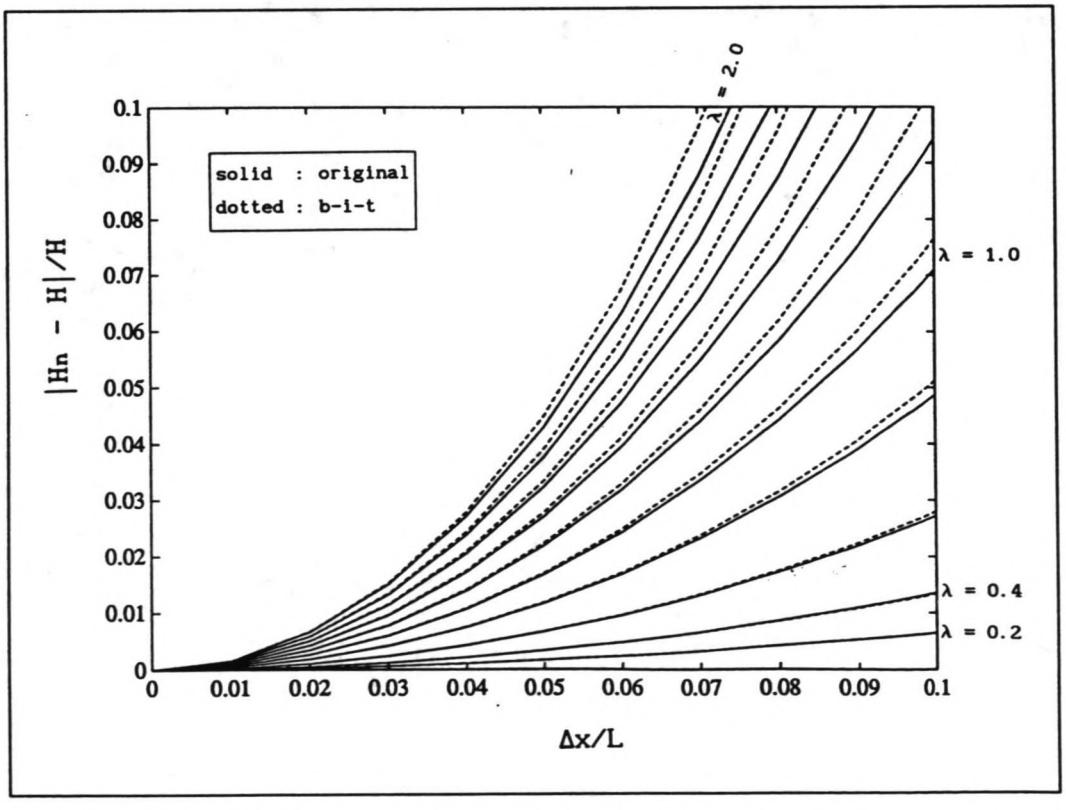

Fig. 5-4: Relative errors of the numerical schemes.

The influence of the convection can be estimated by pushing on the Von Neumann analysis a little further.
Taking again as initial condition :

$$\phi(x,0) = \phi^0 \exp(ikx)$$

the analytical solution becomes (see Vreugdenhil, 1989) :

$$\phi(x,t) = \phi^0 \exp(ik(x-ut))$$

For the back-into-time method this is put into the form :

$$\phi(x,0) = \exp(ikut)\ \phi(x,t) \qquad (5.17)$$

According to the Von Neumann analysis the finite difference solution for the back-into-time scheme reads :

$$\phi(x,t) = \phi^0\ |\rho|^n \exp(ikx + ni\alpha) \qquad (5.18)$$

where α is the argument of the amplification factor ρ given in Eq. (5.11). The ratio of the amplitudes in Eqs. (5.17) and (5.18) after n steps is the damping factor

$$d(n) = |\rho|^n$$

and the ratio of the phase angles is the relative celerity

$$c_r = n\alpha/ukt = \alpha/2\pi\sigma\xi$$

In Fig. 5-5 the relative celerity and the damping factor are given as function of $\Delta x/L$.
It can be concluded that in the back-into-time scheme, shorter waves are also damped more strongly than longer waves, so here too the shortest relevant wave length is the critical one for numerical accuracy.

5.5 Extending the model with dead zones

If the cross-section of the river is extended with dead zones, a set of two differential equations has to be solved (see Section 2.4) :

$$\frac{\partial \phi_s}{\partial t} + u_s \frac{\partial \phi_s}{\partial x} - K_s \frac{\partial^2 \phi_s}{\partial x^2} + D_s(\phi_s - \phi_d) = 0 \qquad (5.19a)$$

$$\frac{\partial \phi_d}{\partial t} - D_d(\phi_s - \phi_d) = 0 \qquad (5.19b)$$

The explicit difference equations are :

$$\frac{\phi s_i^{k+1} - \phi s_i^k}{\Delta t} + u_s \frac{\phi s_{i+1}^k - \phi s_{i-1}^k}{2\Delta x} - K_s \frac{\phi s_{i+1}^k - 2\phi s_i^k + \phi s_{i-1}^k}{\Delta x^2} + D_s(\phi s_i^k - \phi d_i^k) = 0 \qquad (5.20a)$$

$$\frac{\phi d_i^{k+1} - \phi d_i^k}{\Delta t} - D_d(\phi s_i^k - \phi d_i^k) = 0 \qquad (5.20b)$$

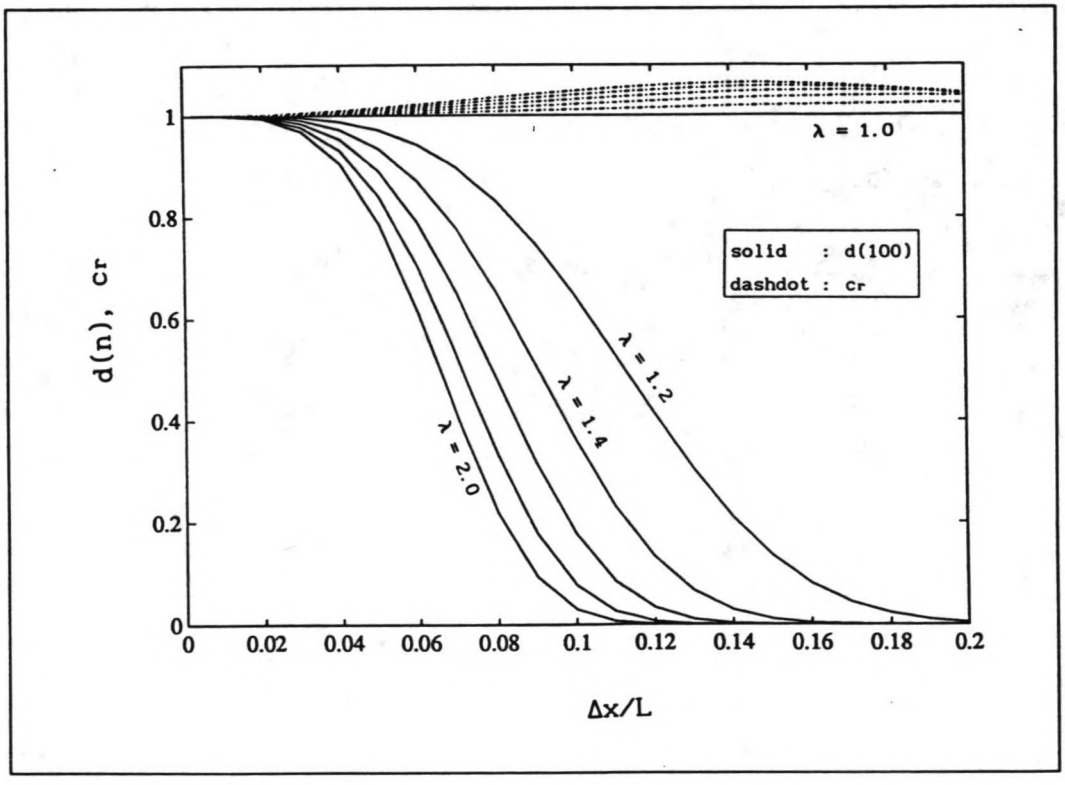

Fig. 5-5: Relative celerity and damping factor (after Noppeney, 1988).

To study the stability of this system, the Von Neumann method is used again. Using the same approach as in Section 5.2, the amplification factors are found to be :

$$\rho_1 = 1 + \lambda(\cos(\xi)-1) + \beta_1(\beta_2-1) - \sigma\, i\, \sin(\xi) \qquad (5.21a)$$

$$\rho_2 = 1 - \beta_2 \qquad (5.21b)$$

with $\beta_1 = \Delta t \, D_s$

$\beta_2 = \Delta t \, D_d$.

With the condition for numerical stability, $|\rho| \leq 1$, the following relations can be derived :

$$\lambda - 1/2 \, \beta_1(\beta_2 - 1) \leq 1 \qquad (5.22a)$$

$$\sigma^2 \leq (1 - (1 + \lambda(\cos(\xi) - 1) + \beta_1(\beta_2 - 1))) \, / \, \sin^2(\xi) \qquad (5.22b)$$

$$\beta_2 \leq 1 \qquad (5.22c)$$

$$0 \leq \beta_2 \leq 2 \quad \text{(condition following from } |\rho_2|^2 \leq 1) \qquad (5.22d)$$

The Figures 5-6 and 5-7 show the conditions (5.22a) and (5.22b) for a few different values and combinations of β_1 and β_2.

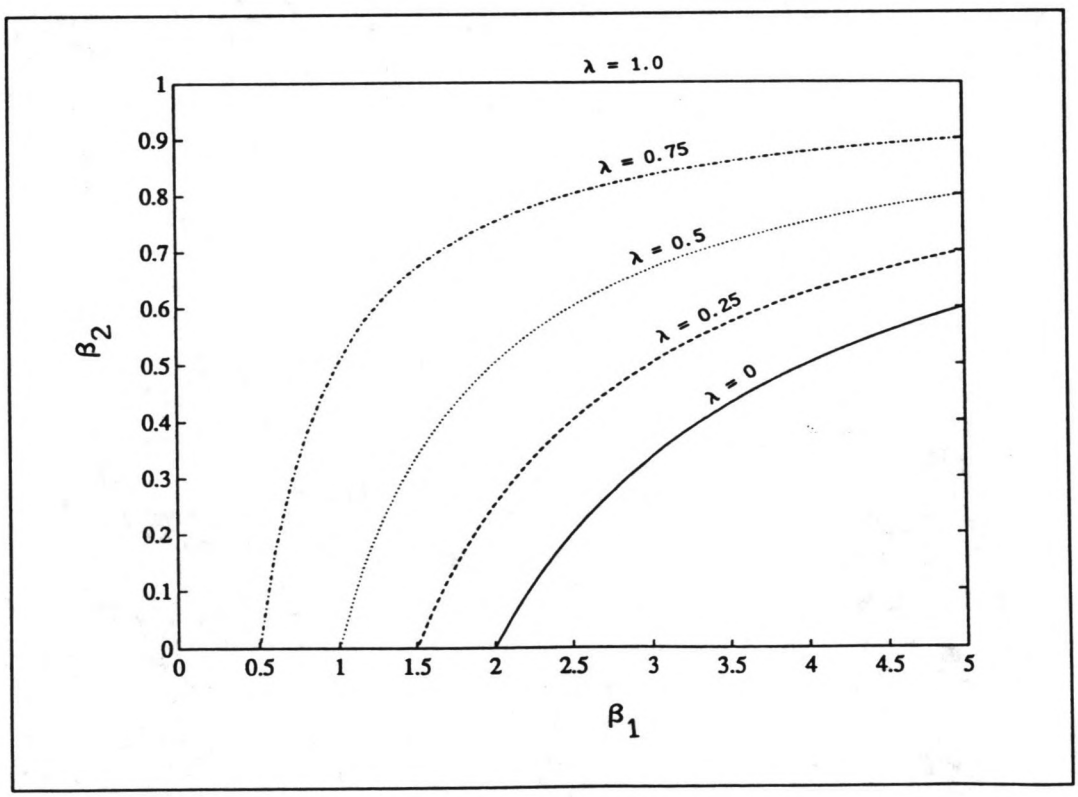

Fig. 5-6: Stability condition for λ, $\beta 1$ and $\beta 2$.

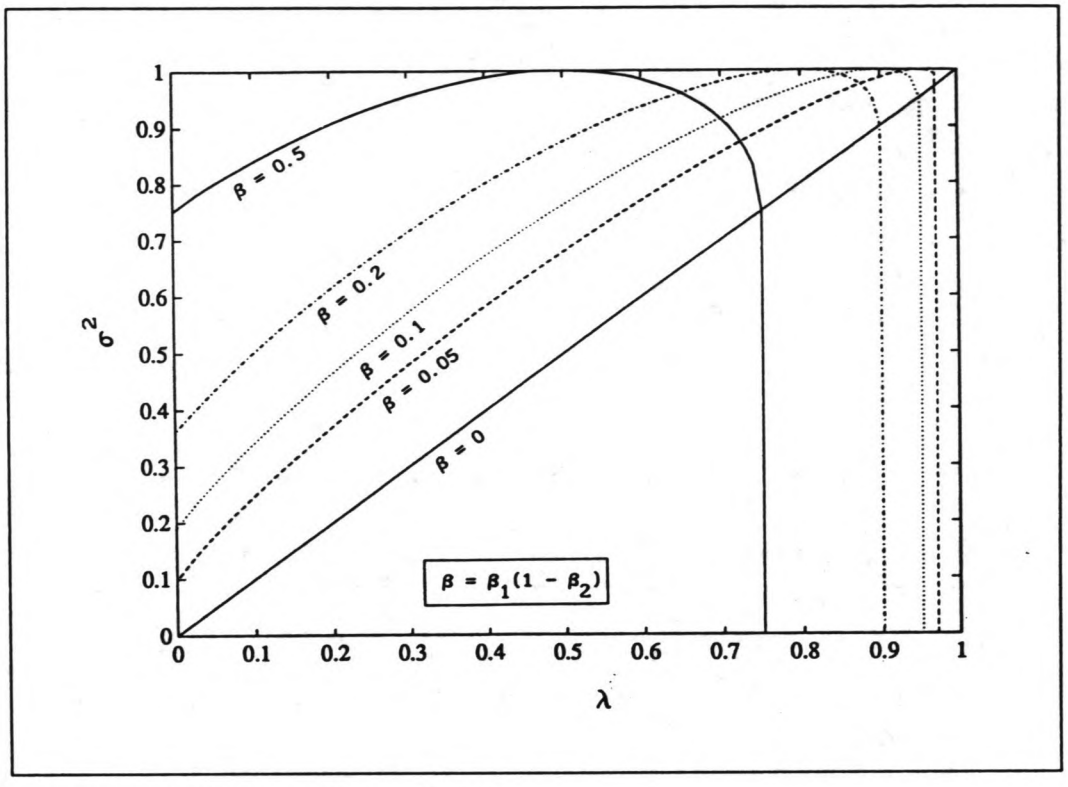

Fig. 5-7: Stability condition (5.22b).

For the back-into-time computation the dead-zone model has to be inverted, but that is here more complicated than in Section 5.2. Writing for example Eq (5.20b) in back-into-time mode , gives :

$$\phi d_i^k = \frac{1}{1 - \beta_2} \phi d_i^{k+1} - \frac{1}{1 - \beta_2} \phi s_i^k$$

Thus the amplification factor for this scheme is :

$$\rho = \frac{1}{1 - \beta_2}$$

and ρ is greater than unity for positive values of β_2, which implies instability. Direct inversion of the dispersion equation for the flow zone also leads to a numerical instabile scheme.

To avoid these instabilities the source term caused by the dead zones is not added to the normal dispersion equation (as is done in Eq. (5.20a)), but to the inverted equation (5.5). For the description of the concentration in the dead zone Eq. (5.20b) is used. So, the back-into-time scheme from Section 5.2 is extended with dead zones, yielding the following model :

$$\underline{X}_k = F\,\underline{X}_{k+1} - \beta_1(\underline{X}_{k+1} - \underline{Xd}_{k+1}) \tag{5.23a}$$

$$\underline{Xd}_k = \underline{Xd}_{k+1} + \beta_2(\underline{X}_k - \underline{Xd}_{k+1}) \tag{5.23b}$$

Now the amplification factors are :

$$\rho_1 = \frac{1 + \beta_1(\beta_2-1) + \beta_1(\beta_2-1)\lambda(\cos(\xi)-1) - \beta_1(\beta_2-1)\sigma i\sin(\xi)}{1 + \lambda(\cos(\xi)-1) - \sigma\, i\, \sin(\xi)} \tag{5.24a}$$

$$\rho_2 = 1 - \beta_2 \tag{5.24b}$$

The stability conditions following from these amplification factors are

$$\sigma^2 \geq \frac{\left[1 + \beta_1(\beta_2-1)(1+\lambda(\cos(\xi)-1))\right]^2 - \left[1 + \lambda(\cos(\xi)-1)\right]^2}{\left[1 - (\beta_1(\beta_2-1))^2\right]\sin^2(\xi)} \tag{5.25a}$$

$$\beta_2 \leq 1 \tag{5.25b}$$

In Fig. 5-8 the stability domain described by Eq. (5.25a), is given for a few values of β_1 and β_2 (notice that here the lower bounds are given).

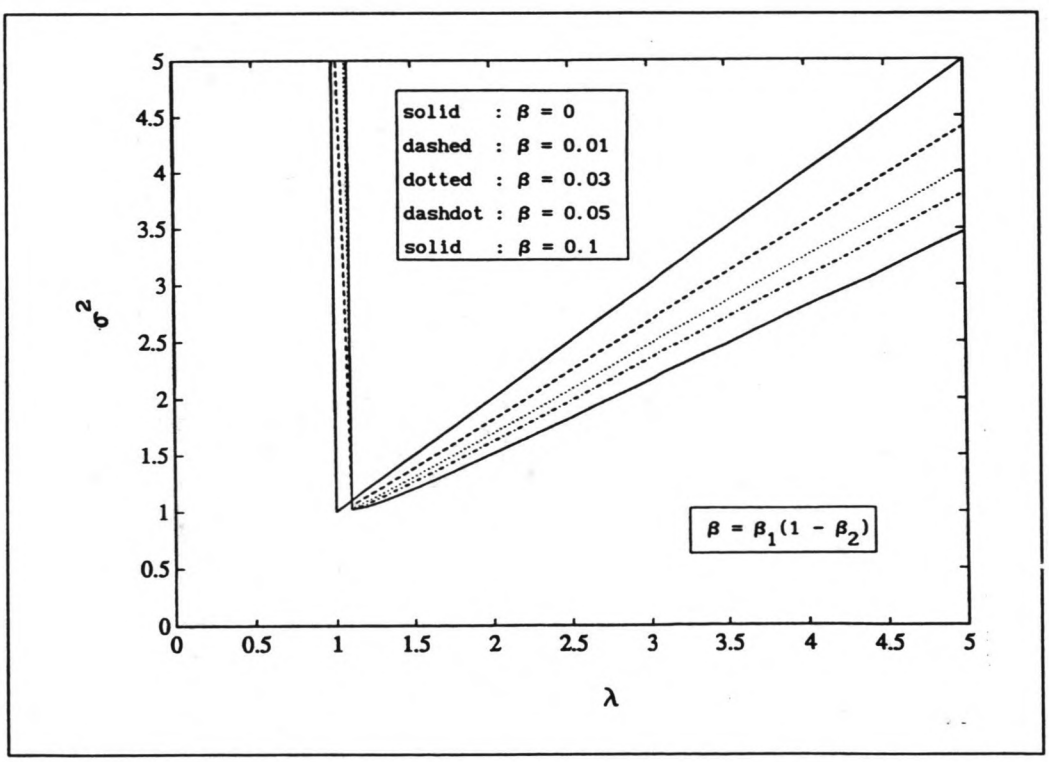

Fig. 5-8: Stability condition for the back-into-time scheme.

Final remark : in the stability and accuracy analyses treated in this Chapter the effect of the Kalman filter was not taken into account while the Kalman filter has definitively much influence in these regions. In fact a Kalman filter is applied to adapt the computations gained with an imperfect model to measurements taken in the real world. Thereby is in Section 4.3 shown that applying a Kalman filter improves the stability of the original system.

CHAPTER 6 NUMERICAL RESULTS

6.1 Introduction

In this Chapter the performance of the back-into-time model is investigated. The approach consists of generating the measurements with a "truth" model (Eq. (5.20)) for the situation that at the upstream boundary (x=0) a flood wave is introduced by way of an appropriate boundary condition. Then the back-into-time model is applied to study its capability to reconstruct the original concentration at x=0. Use of the same boundary condition leads -with the computed concentration- to the discharge looked for.

The advantage of numerical experiments is that the true concentrations, velocities and parameters are known and consequently, model performance can be evaluated quantitatively under a variety of circumstances.

In Section 4.5 has been described how uncertain parameters can be estimated along with the state. The parameters to be considered for the case at hand are K, D_s and D_d. The capability of the model to estimate these uncertain parameters is investigated in Section 6.3.

To be able to compute the original discharge from a set of measured concentrations and the amount of injected tracer material, an iterative back-into-time model is developed and tested in Section 6.4. In this iteration the program Duflow will be used to compute the velocity distribution (Duflow is a micro-computer package for the simulation of one-dimensional unsteady flow in channel systems).

The initial values necessary to start the computation are previously given in Section 6.2.

6.2 Initial values

The river characteristics used in the computation are based on data from the Indonesian river Ciliwung :

river discharge Q = 5 m^3/s,

mean width B = 10 m,
mean velocity v = 0.5 m/s,
Chezy-coeff. C = 35 $\sqrt{m}$/s,
disp. coeff. K = 25 m^2/s,
"mixing length" L = 1 km,

where the "mixing length" is defined as the distance beyond which the released substance is "completely mixed" ($\phi(x,y,z)/\bar{\phi} \geq 0.99$) over the cross-section.
The three different flood waves used in the experiments are shown in Fig. 6-1.

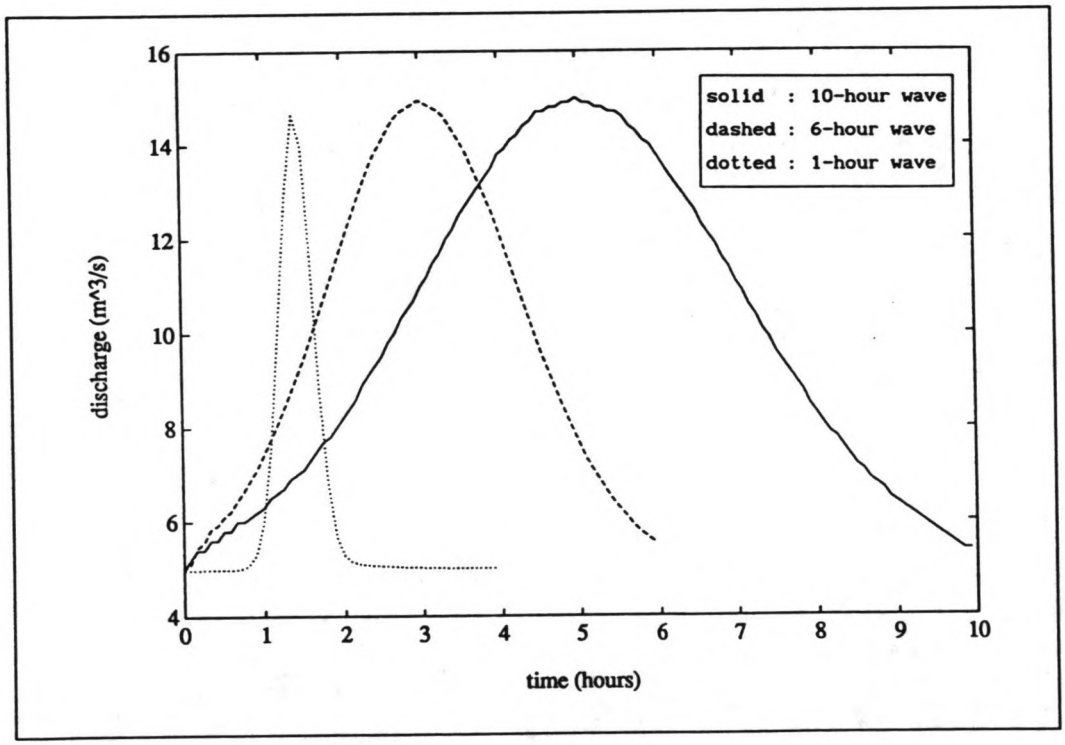

Fig. 6-1: Flood waves used in the computations.

Unless special mention is made, the following values are used in the Kalman filter :

grid size Δx = 100 m,
length of the river section = "mixing length" L = 1000 m,
time step Δt = 5 min,

dead-zone parameters $D_s = 10^{-3}\ s^{-1}$,
$D_d = 5*10^{-3}\ s^{-1}$,
tracer release $M = 0.02\ m^3/s$,
initial concentration $\phi_i = 0$,
system-noise statistics : $\underline{q} = \underline{0}$; $\underline{Q} = 10^{-6}\ I$,
observation-noise statistics : $r = 0$; $R = 10^{-6}$,
initial covariance matrix P_0 is a null matrix.

The discharge is computed with the upstream-boundary concentration using the relation $Q(0,t) = M/\phi(0,t)$ (Eq. (5.2) with $\phi_i = 0$).

The computer program used to solve the dispersion equation back-into-time is given in Appendix C.

6.3 Parameter estimation

Experiment 1 (10-hour flood wave).
In this experiment the influence of the different terms of the dispersion equation (2.4) is investigated. Fig. 6-2 shows the distribution in time of the respective terms 500 m from the point of release (of course not the downstream boundary). It is obvious that the diffusion term has no influence, except for the initial time when the tracer front arrives. This is due to the fact that the grid size Δx is very small with respect to the length of the flood wave which is approximately 50 km.

Experiment 2 (10-hour flood wave).
The influence of the dead zones or the parameters D_s and D_d is investigated in this experiment. The influence of the relation between D_s and D_d is shown in Fig. 6-3, where $D_s = 10^{-4}$ and D_d is 1, 5 and 10 times D_s, respectively.
Fig. 6-4 shows the influence of the values of D_s and D_d.

The experiments 1 and 2 have shown that a change in the value of the

parameters K, D_s and D_d has little or no influence on the computed concentrations. Therefore it does not seem useful to adapt these parameters to the changing conditions during a flood wave.

Reasoning the other way around, the distribution of the concentration does not tell much about the parameters. This and the fact that the concentrations between adjacent grids along the reach L do not differ significantly, keeps us from building a filter which can estimate the parameters along with the concentrations. Consequently it will not be necessary to use a non-linear filter -which is necessary for parameter estimation, see Section 4.5- and a standard Kalman filter is sufficient.

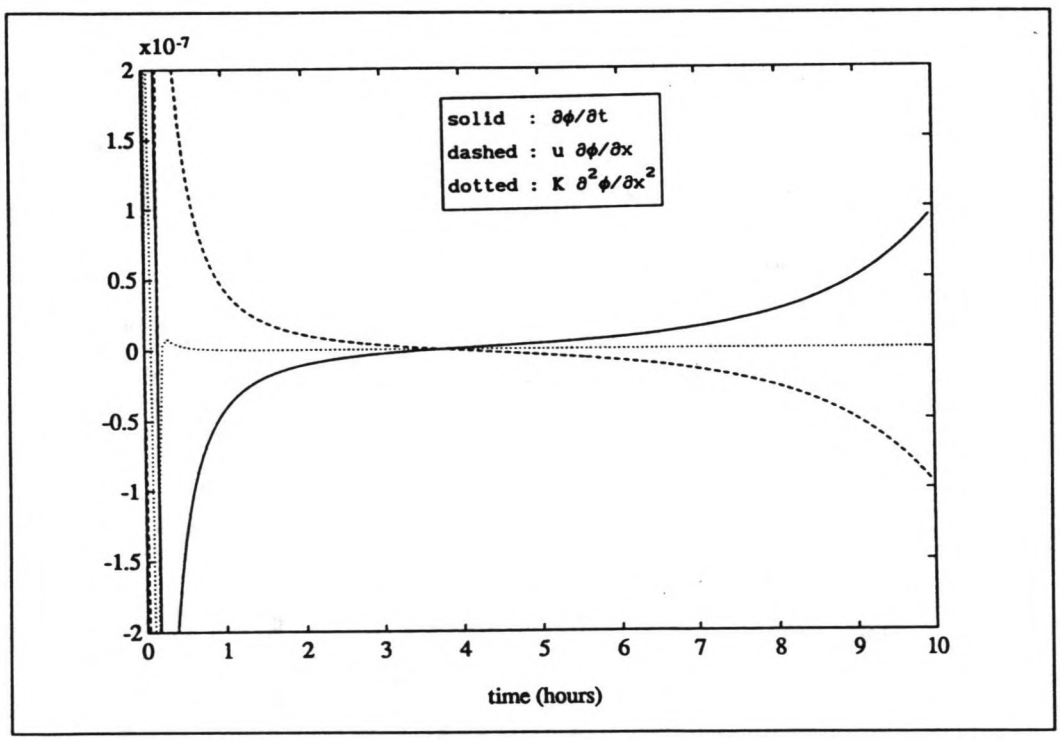

Fig. 6-2: Influence of the terms of the dispersion equation (10-hour flood wave).

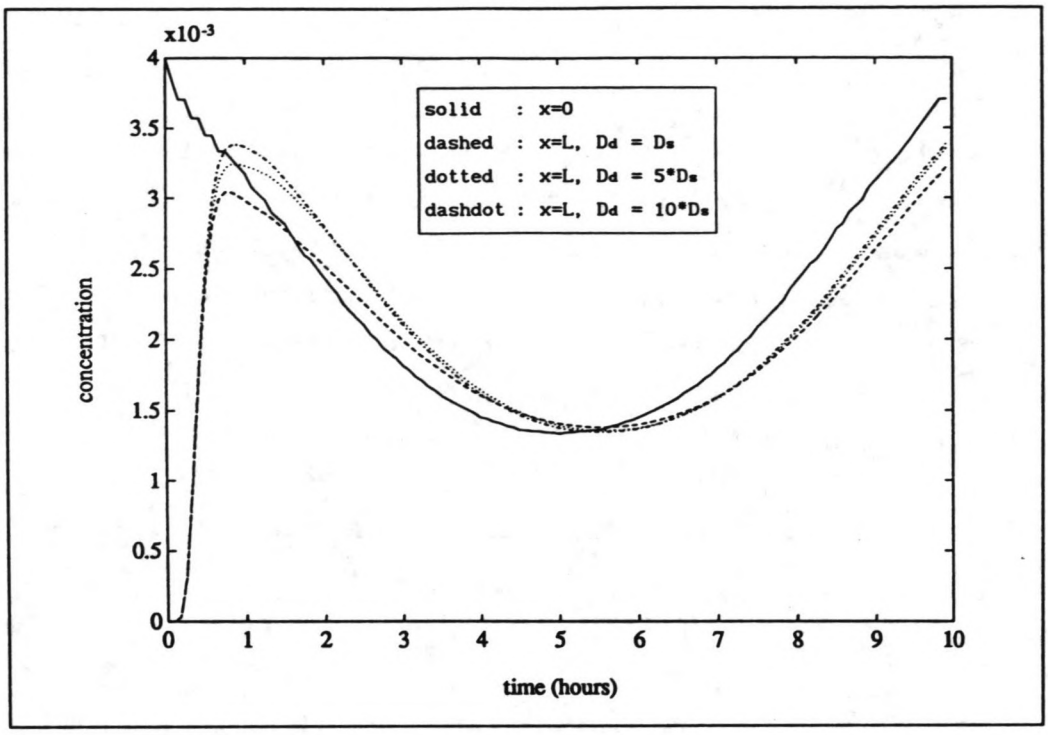

Fig. 6-3: Influence of the relation between Ds and Dd (10-hour flood wave).

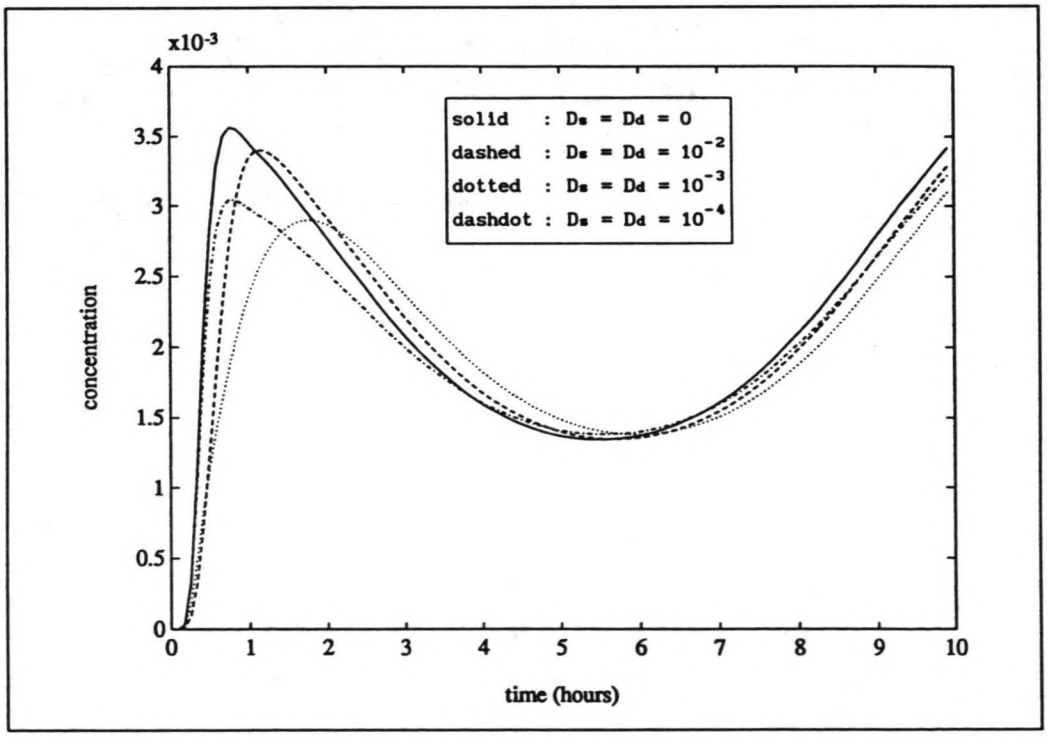

Fig. 6-4: Influence of the value of Ds and Dd (10-hour flood wave).

6.4 Back-into-time model

Experiment 3.

The performance of the model is here tested for a steady flow with a changing release, resulting in the same distribution of the upstream boundary concentration as in the case of a 10-hour flood wave.

Fig. 6-5 shows the upstream and downstream boundary computed with the "truth" model. The upstream concentration computed with the back-into-time (b-i-t) model, which is remarkably close to the original concentration, is also given.

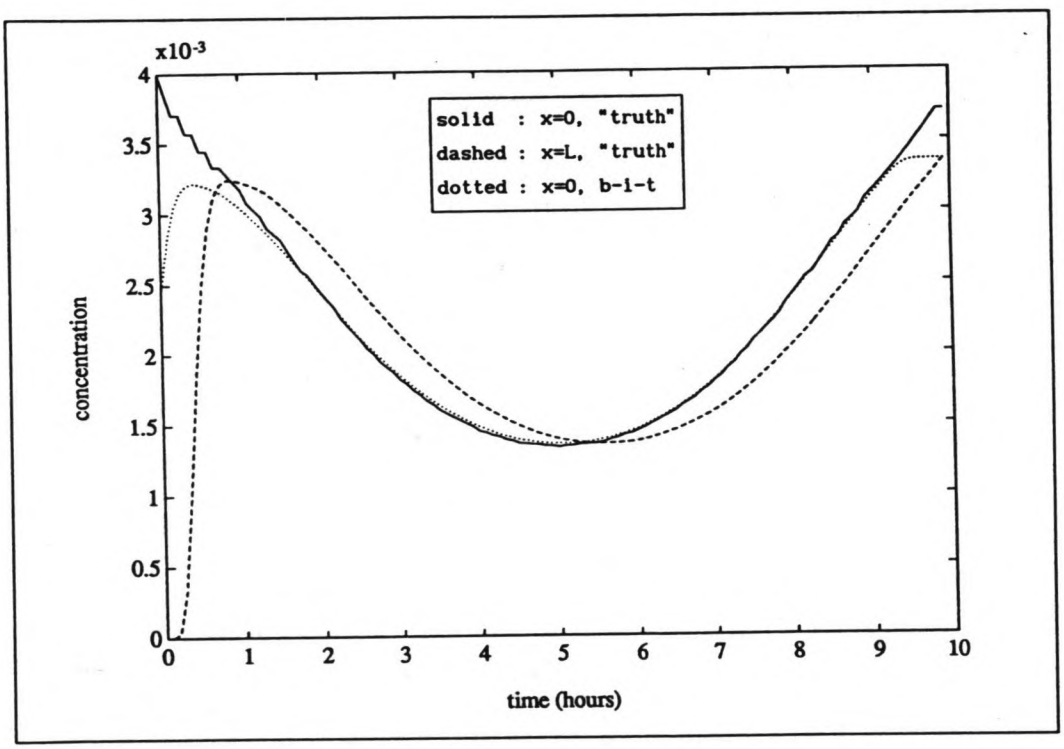

Fig. 6-5: Result using a steady flow with a changing release.

Experiment 4 (10-hour flood wave).

In this experiment the influence of the time step Δt on the accuracy of the b-i-t model is investigated. To avoid a limitation of the time step by stability condition (5.25b), the dead zones are not taken into account (so $D_s = D_d = 0$).

Fig. 6-6 shows the concentrations computed for Δt = 5, 10 and 20 min.

The original concentration is also given. It can be seen that the accuracy of the b-i-t model for Δt = 5 min is of the same order as for Δt = 10 min. For Δt = 20 min the model is less accurate.
In combination with the chosen dead-zone parameters (see Section 6.2), the b-i-t model is not stabile for Δt = 10 min (condition (5.25b)), so Δt = 5 min will be used in the following experiments.

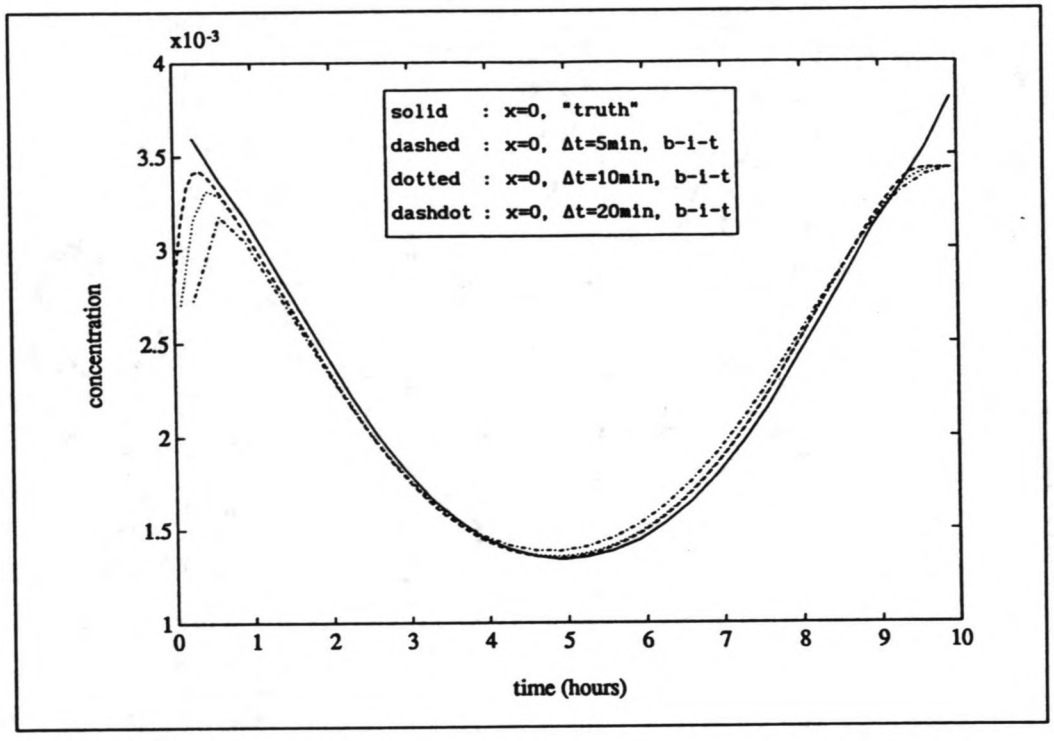

Fig. 6-6: Influence of the time step (10-hour flood wave).

Experiment 5 (10-hour flood wave).
From now on a constant release of tracer material into a simulated flood wave is assumed. The result is a changing velocity (see Fig. 6-7), which is computed with Duflow. Fig. 6-8 shows the concentration computed with the b-i-t model, when the velocity distribution is imposed as a known quantity.

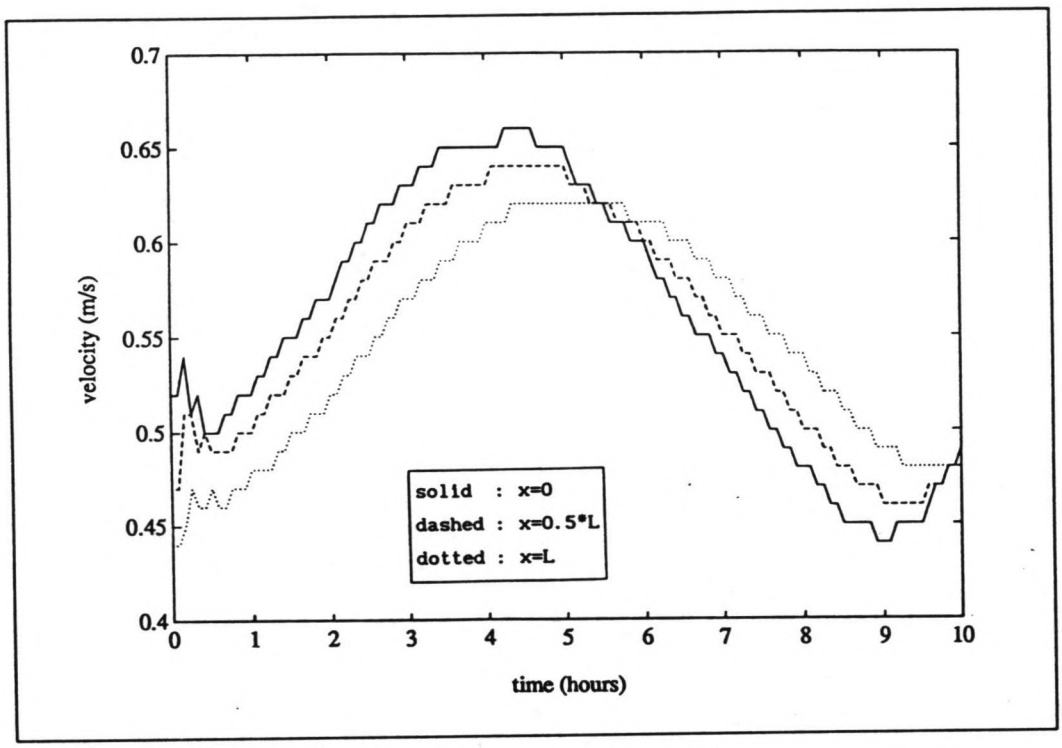

Fig. 6-7: Velocity distribution (10-hour flood wave).

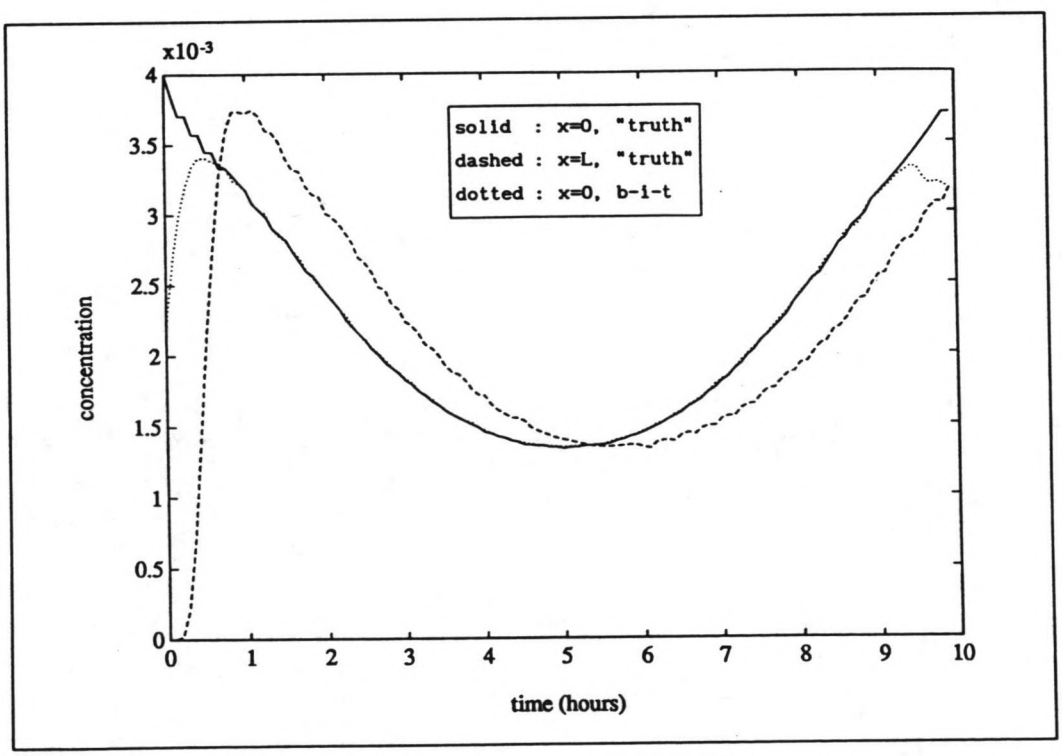

Fig. 6-8: Result when velocity distribution is supposed to be known (10-hour flood wave).

Experiment 6 (10-hour flood wave).

In experiment 5 the velocity distribution was supposed to be known, but in reality this will not be the case. To investigate whether the model can converge to the right solution, the concentrations are determined by an iterative process :

a : estimate the velocity distribution;

b : compute the upstream concentrations with this velocity distribution and the measurements;

c : compute the discharge with these concentrations;

d : compute a new velocity distribution with Duflow and the discharge

e : repeat the steps b, c and d until the discharge does not change anymore.

The Figures 6-9 and 6-10 show that this iterative b-i-t model does converge from both above and below and that reasonably good solutions can be obtained with two or three iterations.

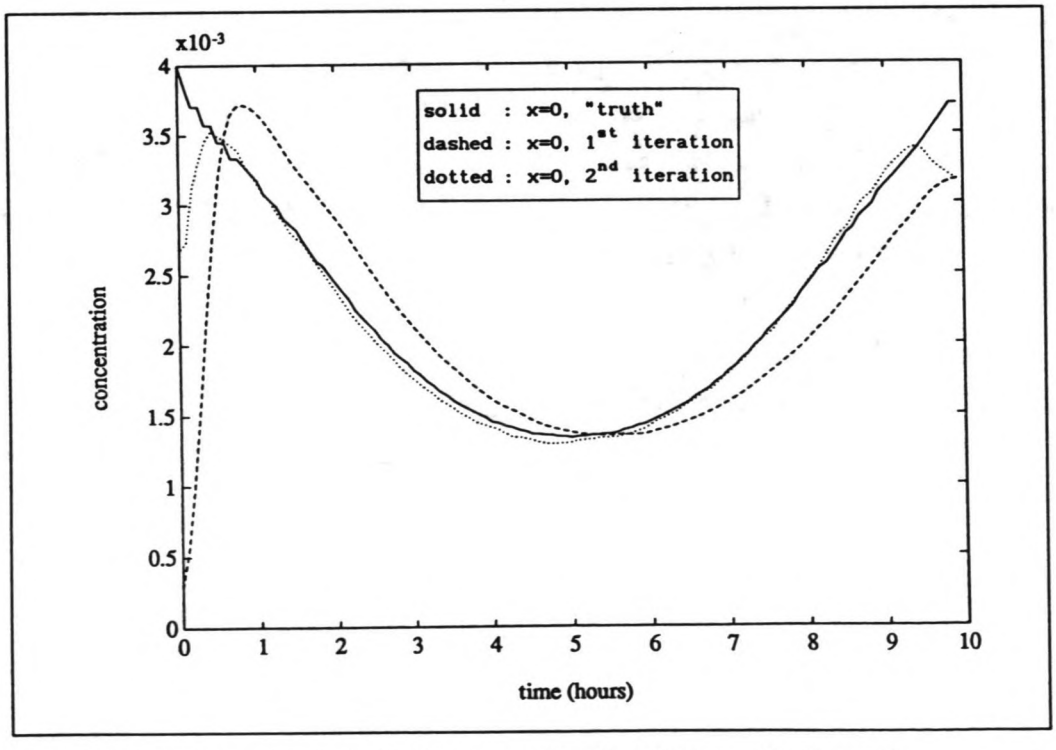

Fig. 6-9: Iteration started with v = 1.5 m/s (10-hour flood wave).

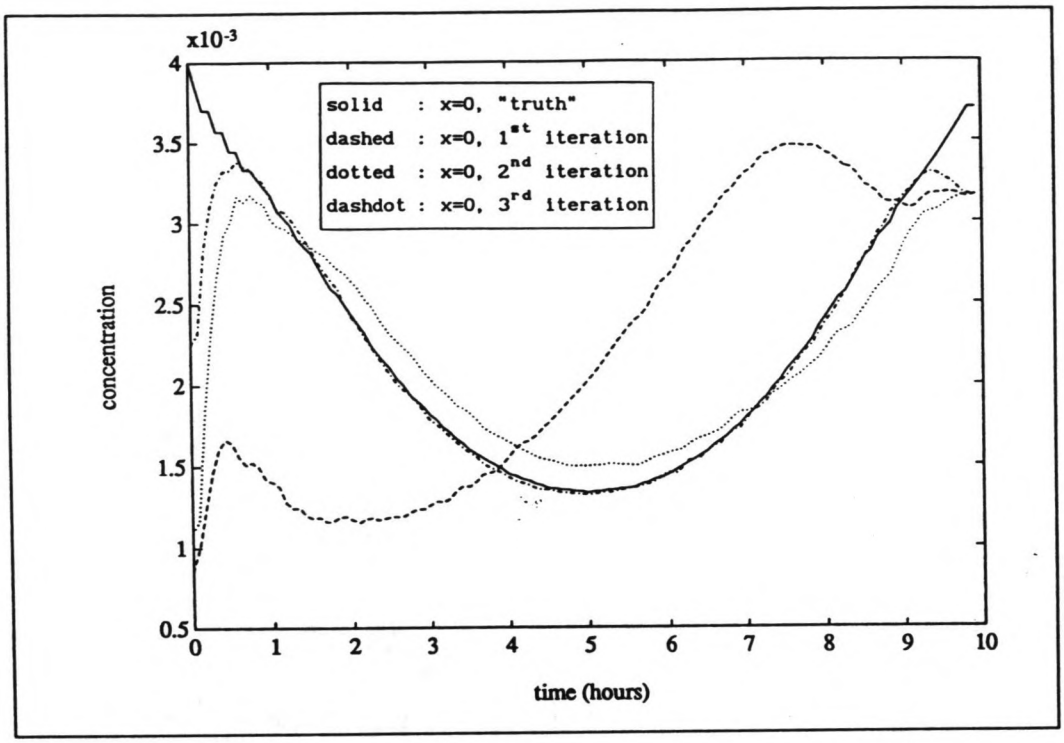

Fig. 6-10: Iteration started with v = 0.1 m/s (10-hour flood wave).

Experiment 7.

In experiment 6 the iteration was started with a velocity distribution which was quite arbitrarily chosen. A good approximation of the discharge, however, can be computed using the measured concentration. Now the iteration can be started at step d. The results of such a computation are shown in Fig. 6-11.

Experiment 8.

In this experiment the concentration is computed in the same way as in experiment 7, but now the 6-hour wave from Fig. 6-1 is used. The results are shown in Fig. 6-12.

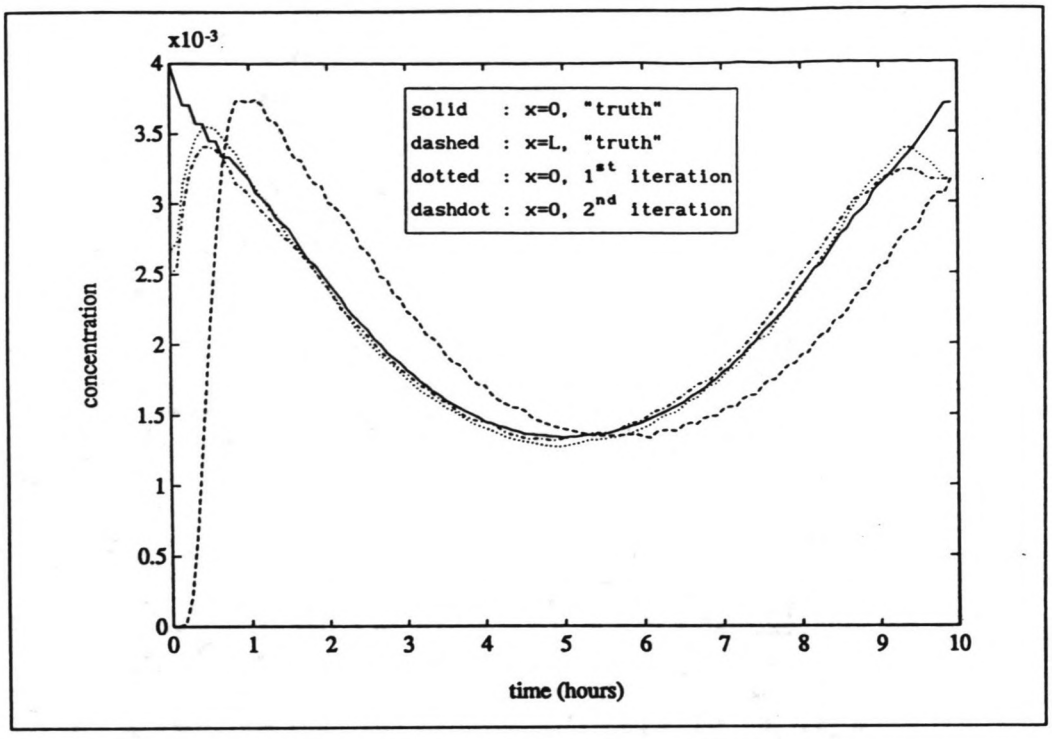

Fig. 6-11: Iteration started with the velocity distribution computed from the measured concentrations (10-hour flood wave).

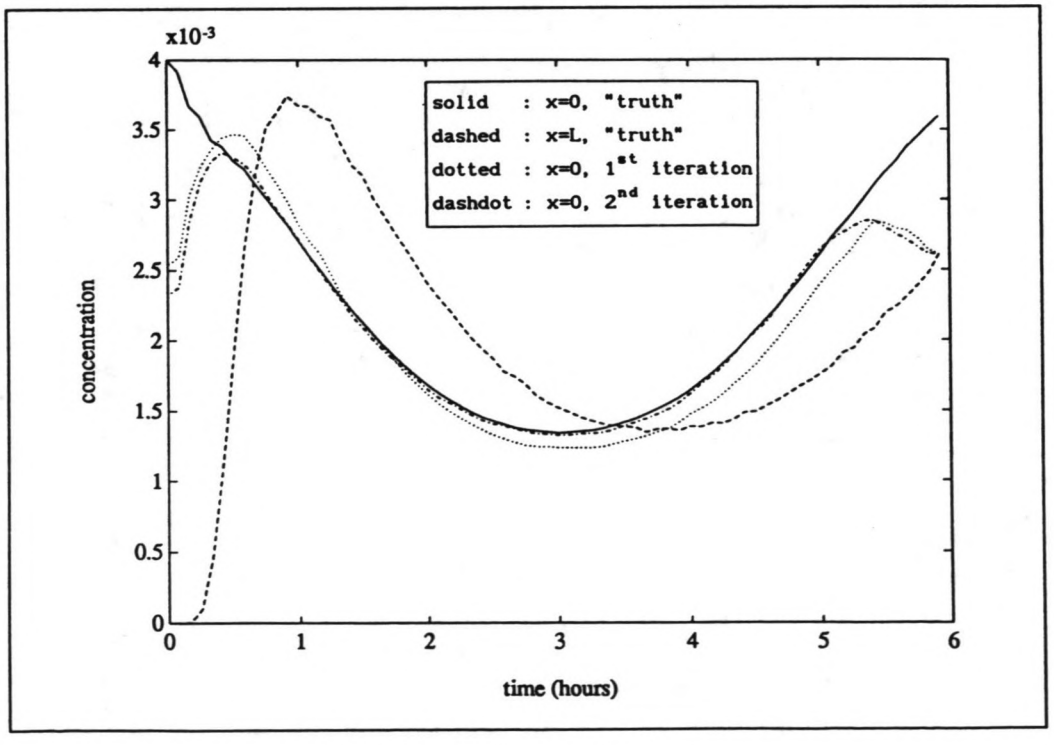

Fig. 6-12: Iteration with a 6-hour flood wave.

Experiment 9 (6-hour flood wave).

Until now the 'measured' concentration was taken equal to the concentration at x=L, computed with the "truth" model. In practice, however, the measured concentration will always have a measurement noise. Therefore, in this experiment, the 'measured' concentration is assumed to have a normal distribution with a mean equal to the concentration computed with the "truth" model and a variance of ten percent of that concentration.

Fig. 6-13 shows the 'measured' concentration together with the concentrations computed with the "truth" model. The results obtained if these 'measured' concentrations are introduced into the iterative b-i-t model, are given in Fig. 6-14.

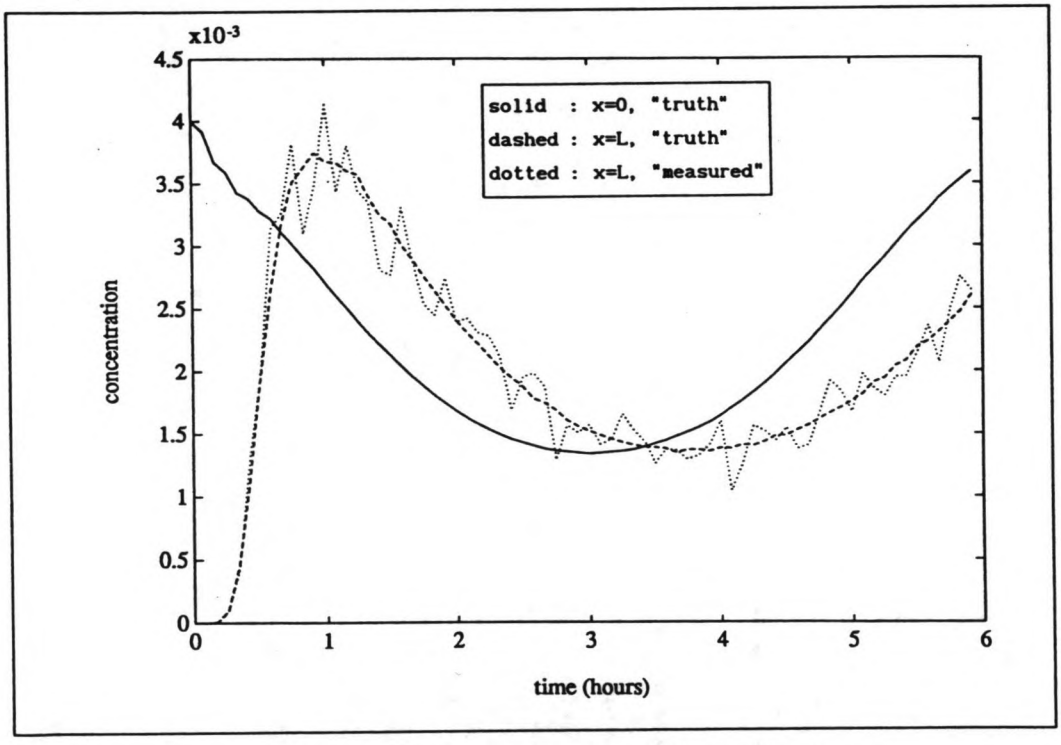

Fig. 6-13: Measurement with measurement noise (6-hour flood wave).

Experiment 10.

To check the validity of the model for shorter waves, the model is also tested for the 1-hour wave given in Fig. 6-1. The results are presented in Fig. 6-15 and show that even such an extreme short flood wave can be computed quite reasonably (in this computation the velocity distribution was presumed to be known).

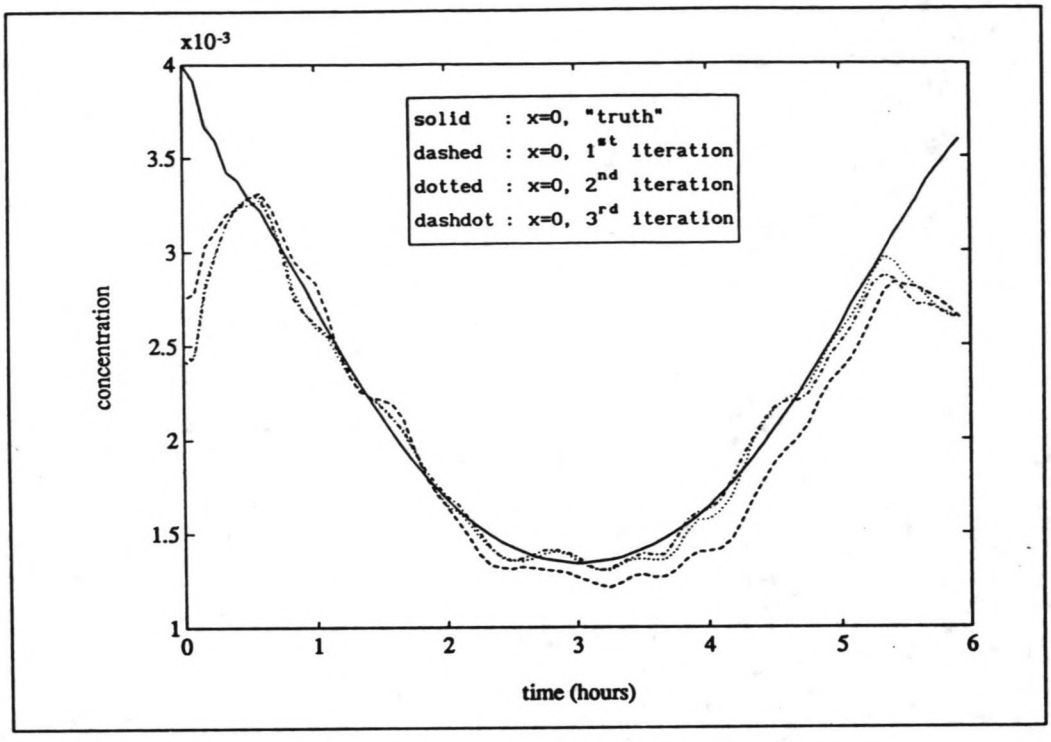

Fig. 6-14: Result obtained in case of measurements with noise (6-hour flood wave).

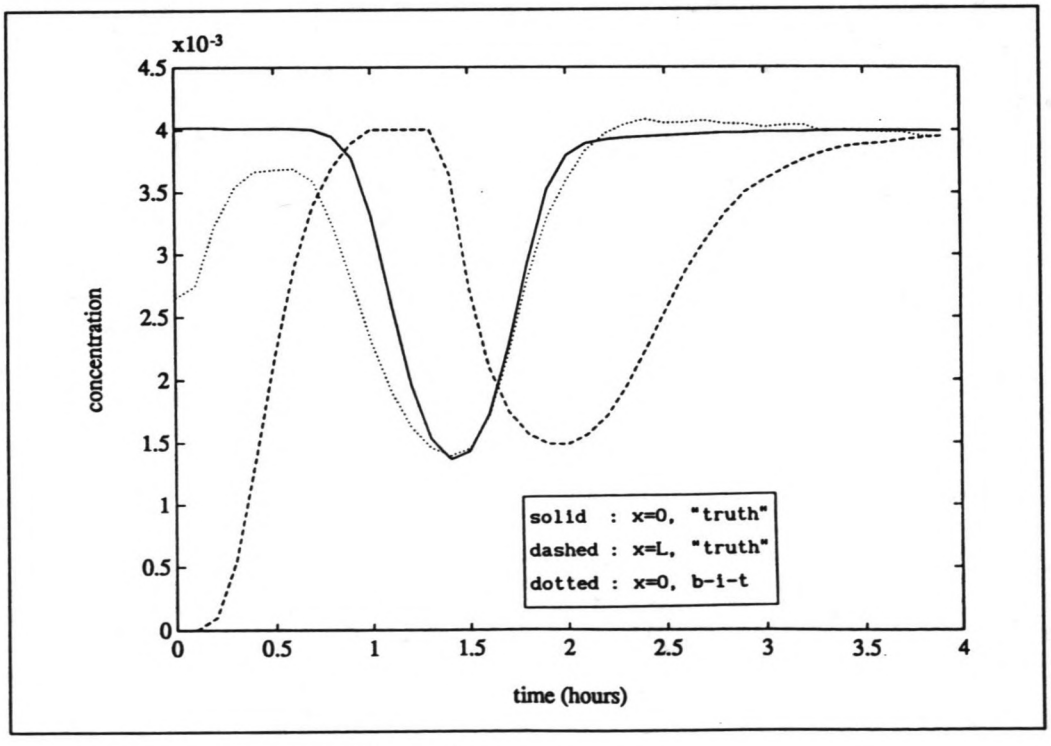

Fig. 6-15: Result for a 1-hour flood wave.

CHAPTER 7 CONCLUSIONS AND RECOMMENDATIONS

The aim of this study was to make the dilution method applicable for mountain-streams under flood wave conditions. Noppeney (1988) has shown that the explicit relation between the concentration of tracer material and the discharge, which can be used in steady flow, is very inaccurate during a flood wave. This is the result of a difference in the respective velocities of propagation between flood wave and tracer cloud and downstream from the point of tracer injection this difference will cause a time lag between the computed discharge and the actual discharge.

The time lag can be avoided if the discharge is computed at the injection point and therefore a method to compute the concentration of tracer material at the injection point is developed in this study.

The developed model is the back-into-time model (b-i-t) and a comparison between the results gained with this model and the values computed with

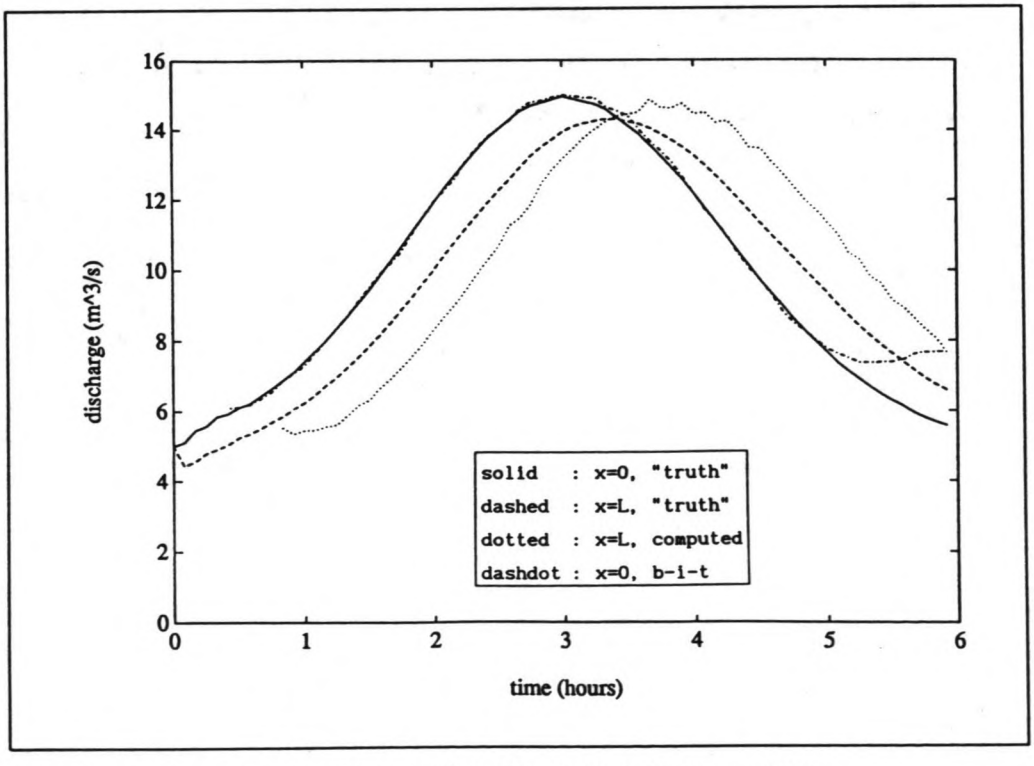

Fig. 7-1: Improvement achieved with the back-into-time model.

the explicit relation for steady flow, are given in Fig. 7-1. In Fig. 7-1 are also given the with a "truth"-model computed actual discharges at the injection point (x=0) and at the measurement point (x=L).

The "truth"-model used to compute the actual discharge and the 'measured' concentrations, is based on the same numerical scheme as is used for the back-into-time model. This yields that the model gives a nearly exact description of the 'reality' and this means that a topic for further study must be the numerical accuracy in modelling the dispersive processes in mountain-streams in the real world.
Another topic is the modelling of flood waves through mountain-streams. Here the program Duflow is used, but Duflow is a micro-computer package for the simulation of one-dimensional unsteady flow in channel systems and it is clear that Duflow cannot deal with the specific problems that are encountered in real mountain-streams.

The results in Fig. 7-1 show that the accuracy problems caused by the time lag can be avoided by using the back-into-time model and when the problems just described can be solved it seems possible to make the dilution method applicable for the determination of discharges in mountain-streams under flood wave conditions.

LIST OF SYMBOLS

All symbols are explained when they first appear in the text. In case of non-uniqueness of symbols; their meaning is clear from the text.

Symbol	Definition	Dimension
A	cross-sectional area of the river	L^2
a	mean flow depth	L
B	mean flow width	L
C	Chezy-coefficient	$L^{1/2}T^{-1}$
cr	relative celerity	LT^{-1}
$\mathcal{C}$	controllability matrix	--
D	exchange velocity	LT^{-1}
D_d	entrainment coefficient	T^{-1}
D_s	entrainment coefficient	T^{-1}
d(n)	damping factor	--
F	mass-flux	$ML^{-2}T^{-1}$
	Φ^{-1} = inverse of the state transition matrix	--
f	friction factor	--
G	noise input matrix	--
H	observation matrix	--
I	identity matrix	--
K	dispersion coefficient	L^2T^{-1}
	Kalman gain vector	--
k	wave-number	L^{-1}
L	distance from injection point to point of measurement	L
	wave length	L
M	amount of released tracer material	L^3T^{-1}
N	number of grid points	--
n	number of time steps	--
$\mathcal{O}$	information matrix	--
P	cell-Peclet number	--
	state-covariance matrix	--

$Q(x,t)$	discharge at place x and time t	L^3T^{-1}
Q	system noise covariance matrix	--
$\underline{q}$	mean of the system-noise	--
R	observation noise covariance matrix	--
r	mean of the observation noise	--
t	time	T
u	flow velocity in x-direction	LT^{-1}
u^*	shear velocity	LT^{-1}
$\underline{V}$	observation-noise vector	--
$\underline{W}$	system-noise vector	--
$\underline{X}$	state vector	--
x	coordinate along the river axis	L
$\underline{Z}$	observation vector	--
β	dimensionless dead zone parameter	--
Δt	time step	T
Δx	grid size	L
θ	weighting factor	--
λ	diffusion parameter	--
ρ	amplification factor	--
σ	Courant number	--
Φ	state transition matrix	--
ϕ	concentration	--
ϕ_i	initial concentration	--
ϕ_m	measured concentration	--
ϕ_i^k	approximation of $\phi(i\Delta x, k\Delta t)$	--

index	denotes
d	dead zone
k	at time $k\Delta t$
s	flow zone
$\hat{}$	predicted value
$^{-1}$	(matrix) inverse

REFERENCES

Abramowitz, M. and I.A. Stegun (1965)
'Handbook of mathematical functions'
Dover Public. Inc., New York.

Anderson, B.D.O. and J.B. Moore (1979)
'Optimal filtering'
Prentice-Hall, Englewood Cliffs, New Jersey.

Berkhoff, J.C.W. (1973)
'Transport of pollutants or heat in a system of channels'
in: Proc. Tech. Meeting 26
'Hydraulic research for water management'
Committee for hydrological research TNO, The Hague.

Chao-Lin Chiu (ed.) (1978)
'Applications of Kalman filter theory to hydrology, hydraulics and water resources'
University of Pittsburg, Pittsburg.

Chao-Lin Chiu and E.O. Isu (1978)
'Stream temperature estimation using Kalman filter theory'
Journal of the Hydraulics Division ASCE, Vol. 104, No. HY9.

Day, T.J. (1975)
'Longitudinal dispersion in natural channels'
Wat. Resour. Res., Vol. 11, No. 6, pp 909-918.

Fischer, H.B. et al. (1979)
'Mixing in inland and coastal waters'
Academic Press, New York.

Heemink, A.W. (1986)
'Storm surge prediction using Kalman filtering', Ph.D. Thesis
Rijkswaterstaat, The Hague.

ISO (1990)
'Liquid flow measurements in open channels. Dilution methods for measurement of steady flow (International Standard ISO 555-1973).

Jansen, P. et al. (1979)
'Principles of river engineering'
Pitman, London.

Jazwinski, A.H. (1970)
'Stochastic processes and filtering theory'
Academic Press, New York.

Kalman, R.E. (1960)
'A new approach to linear filtering and prediction problems'
Journal of Basic Engineering ASME, Vol. 82.

Kalman, R.E. and R.S. Bucy (1961)
'New results in linear filtering and prediction theory'
Journal of Baasic Engineering ASME, Vol. 83.

Maybeck, P.S. (1979)
'Stochastic models, estimation and control', Vol. 1
Academic Press, New York.

Maybeck, P.S. (1982)
'Stochastic models, estimation and control', Vol. 2
Academic Press, New York.

Myers, K.A. and B.D. Tapley (1976)
'Adaptive sequential estimation with unknown noise statistics'
IEEE Transactions on Automatic Control, Short paper.

Noppeney, R.M. (1987)
'Applicability of dilution discharge measurements during flood wave conditions', M.Sc. Thesis
Delft University of Technology, Delft.

Noppeney, R.M. (1988)
'Gevoeligheidsonderzoek Alarmmodel Rijn. De invloed van stagnante zones op dispersie', (in Dutch)
Delft University of Technology/Rijkswaterstaat, Delft.

Nordin, C.F. and B.M. Troutman (1980)
'Longitudinal dispersion in rivers: the persistence of skewness in obsered data'
Wat. Resour. Res., Vol. 16, No. 1.

Purnama, A. (1988)
'The effect of dead zones on longitudinal dispersion in streams'
Journal of Fluid Mech., Vol. 186.

Sage, A.G. and J.L. Melsa (1971)
'Estimation theory with applications to communications and control'
McGraw-Hill Book Co. Inc., New York.

Taylor, G.I. (1954)
'The dispersion of matter in turbulent flow through a pipe'
Proc. R. Society London Ser. A 223.

Thackston, E.L. and K.B. Schnelle (1970)
'Predicting effects of dead zones on stream mixing'
Journal of the Sanit. Engineering Division ASCE, Vol. 96, No. SA2.

Valentine, E.M. and I.R. Wood (1977)
'Longitudinal dispersion with dead zones'
Journal of the Hydraulics Division ASCE, Vol. 103, No. HY9.

Valentine, E.M. and I.R. Wood (1979)
'Experiments in longitudinal dispersion with dead zones'
Journal of the Hydraulics Division ASCE, Vol. 105, No. HY8.

Verwoerdt, P. (1989)
'De één-dimensionale dispersievergelijking van Taylor bij een opdeling van een rivier in vakken', M.Sc. Thesis (in Dutch)
Delft Univ. of Technology, Delft.

Vreugdenhil, C.B. (1985)
'Numerieke berekeningen in waterbouwkunde en hydrologie'
Lecture notes b84N (in Dutch)
Dep. of Civil Engineering, Delft Univ. of Technology, Delft.

Vreugdenhil, C.B. (1989)
'Computational Hydraulics, an introduction'
Springer-Verlag, Berlin.

Vries, M. de (1984)
'Vloeistofmechanica', Lecture notes b71N (in Dutch)
Dep. of Civil Engineering, Delft Univ. of Technology, Delft.

APPENDIX A1 : Observability

The concept of observability is developed to check whether the incorporation of the observation $\underline{Z}_k$ improves the estimates of all the components of the state vector $\underline{X}_k$.
Suppose the system model to be noise-free, i.e. $\underline{W}_k=0$ for all k. In that case, applying some clever algebra (Maybeck, 1979), the equation to compute the covariance matrix P_k can be rewritten as :

$$P_k^{-1} = \Phi^T P_0^{-1} \Phi + \sum_{i=1}^{k} \Phi^T H^T R^{-1} H \Phi \qquad \text{(A1-1)}$$

The information matrix is defined as :

$$\mathcal{O}(k,k-N_1) = \sum_{i=k-N1}^{k} \Phi^T H^T R^{-1} H \Phi \qquad 0 \le N_1 \le k \qquad \text{(A1-2)}$$

where $\mathcal{O}(k,k-N_1)$ = information matrix,
N_1 = integer.

The system model is now said to be uniformly completely observable if there exists a positive integer N_1 and positive constants c_1 and c_2 such that :

$c_1 I \le \mathcal{O}(k,k-N_1) < c_2 I$, for all $k > N_1$

where I = identity matrix.

Observability guarantees that the entire state $\underline{X}_k$ can be determined from the data and prevents that certain eigenvalues of the covariance matrix can grow unrestricted. It also implies that the effects of changes in any component of the state can be observed in the observations.

APPENDIX A2 : Controllability

The controllability of a filter can be checked under the assumption that no observations are available. The equation to compute the covariance matrix P_k then reduces to :

$$P_k = \Phi P_0 \Phi^T + \sum_{i=1}^{k} \Phi G Q G^T \Phi^T \qquad \text{(A2-1)}$$

The controllability matrix is defined by :

$$\mathcal{C}(k, k-N2) = \sum_{i=k-N2}^{k} \Phi G Q G^T \Phi^T \qquad 0 \leq N2 \leq k \qquad \text{(A2-2)}$$

where $\mathcal{C}(k, k-N2)$ = controllability matrix,

N2 = integer.

The system model is now said to be uniformly completely controllable if there exists a positive integer N2 and positive constants c_3 and c_4 such that :

$c_3 I \leq \mathcal{C}(k.k-N2) \leq c_4 I$, for all $k > N2$.

Controllabilty implies that the system noise $\underline{W}_k$ effects all the components of the state $\underline{X}_k$ and prevents certain components of the state to be determined almost exactly, in which case the new observations would have very little effect on the estimates of these components and the estimates and observations could easily diverge. This problem is known as filter divergence.

If a filter is not controllable, numerical difficulties are also very likely to occur. In that case some state components (or linear combinations of the state components) can be estimated very accurately and some eigenvalues of the covariance matrix become almost zero. Due to the finite word length on the computer these eigenvalues can easily become negative, a condition which is theoretically impossible and usually leads to a total failure of the recursion.

APPENDIX B : Nonlinear filtering theory

Consider a filtering problem involving a continuous-time system with discrete-time measurements. Assume that a linear model does not provide a valid description of the problem, i.e., that nonlinearities in the deterministic portion of the state dynamics and measurement models are not negligible.
Suppose the system state and the observations can be described by the nonlinear stochastic equations

$$\underline{X}_{k+1} = f[\underline{X}_k] + G\,\underline{W}_{k+1} \tag{B-1}$$

$$\underline{Z}_k = h[\underline{X}_k] + \underline{V}_k \tag{B-2}$$

in which : $f[\underline{X}_k]$ = nonlinear vector function,

$h[\underline{X}_k]$ = nonlinear state-observation relation.

The other model assumptions are completely similar to those for the linear case treated in Section 4.2.

Suppose now that it is possible to generate a discrete reference state-trajectory $\bar{\underline{X}}_k$. The state equation (B-1) may then be rewritten as (see Heemink, 1986) :

$$\underline{X}_{k+1} = \left\{ f[\underline{X}_k] - f[\bar{\underline{X}}_k] \right\} + f[\bar{\underline{X}}_k] + G\,\underline{W}_{k+1} \tag{B-3}$$

and the observation equation (B-2) as :

$$\underline{Z}_k = \left\{ h[\underline{X}_k] - h[\bar{\underline{X}}_k] \right\} + h[\bar{\underline{X}}_k] + \underline{V}_k \tag{B-4}$$

If the deviation $\underline{X}_k - \bar{\underline{X}}_k$ from the reference trajectory is small, a Taylor series expansion of the terms between braces yields :

$$f[\underline{X}_k] - f[\bar{\underline{X}}_k] \cong F_k\,(\underline{X}_k - \bar{\underline{X}}_k) \tag{B-5}$$

$$h[\underline{X}_k] - h[\bar{\underline{X}}_k] \cong H_k\,(\underline{X}_k - \bar{\underline{X}}_k) \tag{B-6}$$

where respectively

$$F_k = \left. \frac{\partial f[\underline{X}_k]}{\partial \underline{X}_k} \right|_{\underline{X}_k = \bar{\underline{X}}_k} \tag{B-7}$$

$$H_k = \left. \frac{\partial h[\underline{X}_k]}{\partial \underline{X}_k} \right|_{\underline{X}_k = \bar{\underline{X}}_k} \tag{B-8}$$

are the matrices of the partial derivatives along the reference trajectory.

The equations (B-5) and (B-6) can be used to obtain the approximate linear state and observation equations

$$\underline{X}_{k+1} = F_k (\underline{X}_k - \bar{\underline{X}}_k) + f[\bar{\underline{X}}_k] + G \underline{W}_{k+1} \tag{B-9}$$

$$\underline{Z}_k = H_k (\underline{X}_k - \bar{\underline{X}}_k) + h[\bar{\underline{X}}_k] + \underline{V}_k \tag{B-10}$$

and the standard Kalman filter described in Section 4.2 is directly applicable to these linearized equations.

The remaining problem is the choice of the reference (or nominal) trajectory. The obvious choice is made with $\bar{\underline{X}}_0 = \hat{\underline{X}}_0$, the prior estimate of the state and necessary to start the computation. But the new estimates of the state will in general deviate from the prior estimate as we process the observations and the initially wise choice of a reference trajectory may turn out to be a poor one. This will be especially true if P_0 is large (so that $\hat{\underline{X}}_0$ is not a good estimate), and/or if the system noise is large. In that case, the deviation $\underline{X}_k - \hat{\underline{X}}_k$ can become large, violating the linearity assumption.

The estimator just described is called the Linearized Kalman filter.

The basic idea of the Extended Kalman filter (widely used in orbid determination) is to relinearize about each estimate as new estimates become available. This procedure goes as follows. At t_0, linearize about $\hat{\underline{X}}_0$. Once $\underline{Z}_1$ is processed, relinearize about $\hat{\underline{X}}_1$, and so on. The point of this is to use a better reference trajectory as soon as one is available. As a consequence of relinearization, large initial estimation errors are not allowed to propagate through time, and therefore are the linearity assumptions less likely to be violated.

APPENDIX C : Back-into-time computer program

The computer program used to solve the dispersion equation back-into-time is given on the next page. This program is written in MatLab which stands for MATrix LABoratory.
MatLab was originally written to provide easy access to matrix software but has evolved to a versatile scientific "spreadsheet" for numeric calculations and has proven to be a powerful tool in the development of numerical models.

The back-into-time program needs two data input-files:

- -the first must contain a vector with the measured concentrations, and
- -the second must contain a matrix with the predicted velocity distribution.

The boundary conditions are embedded in the state transition matrix, but it is important to note that the upstream boundary must be the injection point and has to be treated as an autoregressive variable, and that the measurement point must be the downstream boundary.

A null matrix can be taken as initial condition for the covariance matric P_0, but this implies that it will take the filter some time to adapt itself to the case in question. The result is that the filter may oscillate in this adaptation time, but these oscillations will damp out as the filter gets better conditioned. To avoid serious oscillations, it is mostly sufficient when the numerical scheme satifies the stability conditions given in Chapter 5. After the adaptation time are those conditions not so harsh anymore through the stabilizing effect of the Kalman filter.

```
% BACK-INTO-TIME PROGRAM

clear                    % Clear memory
deltax = 100;            % Grid size
deltat = 300;            % Time step
lo     = 0.02;           % Tracer release
l      = 1000;           % Length of the river section
k      = 25;             % Dispersion coefficient
Ds     = 1E-3;           % Entrainment coefficients
Dd     = 5E-3;           %

n = fix(l/deltax);          % Number of grid points
la = 2*k*deltat/deltax^2;     % Diffusion parameter

H = zeros(1,n); H(1,n) = 1;        % Observation matrix
P = zeros(n);                      % State-covariance matrix
Q = 1e-6*diag(ones(n,1));          % System noise covariance matrix
R = 1e-6;                        % Observation noise covariance matrix
load truth                     % Load data "truth"-model
Z = downstr;       % Fill observation vector with data from "truth"-model
load V             % Load velocity distribution from Duflow

X = Z(120)*ones(n,1);  % Starting values of all the concentrations in state
Xd = X;                % and dead zones are equal to the last observation

for i=120:-1:1

  u = V(i,:)';
  sigma = u*deltat/deltax;     % Courant number

  F = zeros(n); F(1,1) = 1;                          %
  for j=2:n-1;                                       %
    F(j,j-1) = 0.5*sigma(j-1)+0.5*la;                % Computation of the
    F(j,j) = 1-la;                                   % state transition
    F(j,j+1) = -0.5*sigma(j+1)+0.5*la;               % matrix F
  end                                                %
  F(n,n-1) = sigma(n-1); F(n,n) = 1-sigma(n);        %

  F = inv(F);              % Inversion of F to back-into-time mode

  P = F*P*F' + Q;                          %
  X = F*X - (X-Xd)*deltat*Ds;              %
  K = P*H'*inv(R + H*P*H');                % Filter equations
  P = P - K*H*P;                           %
  X = X + K*(Z(i) - H*X);                  %
  Xd = Xd + (X-Xd)*deltat*Dd;              %

  pd1(i) = X(1);               % Store interesting data
  pdn(i) = X(n);               %

end
```